DOI: 10.24427/978-83-65596-73-4_2

2. SOLAR SYSTEMS

2.1. Solar irradiation

The Sun, as any other active star, is a giant fusion reactor in which every second are generated 600 million tons of helium through the proton-proton cycle, which can be synthesized in the following reaction: $4p \rightarrow {}^{4}He + 2e^{-} + \nu_e + 26.2MeV$. These processes of nuclear fusion release heating capacity evaluated as $3.86 \cdot 10^{23}$ kWth.

For the exploitation of this energy it is possible to consider the sun as a black body that radiates energy at a temperature of 5780K, because its spectral distribution is very similar to that of the black body for the wavelength range typical of the thermal and photothermic processes.

In Fig. 2.1, there has been presented the spectral distribution of the extraterrestrial radiation and the spectral distribution of the radiation at the sea level.

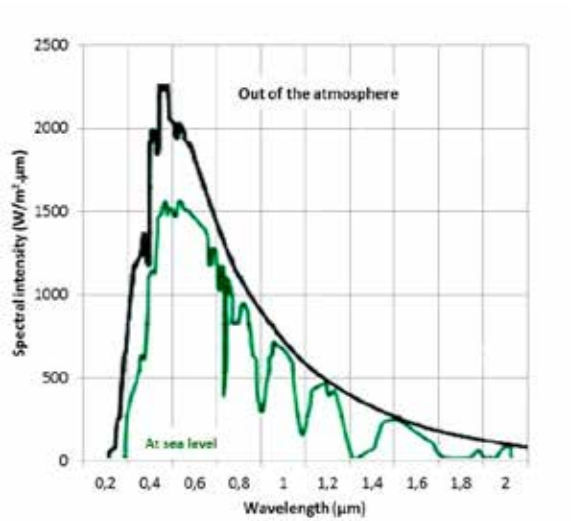

Fig. 2.1. Intensity of the solar spectrum as a function of the wavelength (Source: Martínez-Val, 2004)

The solar radiation can decompose according to thermal considerations in the spectrum:

- ULTRAVIOLET (UV) $\lambda < 0.35$ nm 7% transported energy,
- VISIBLE 0.35 nm $< \lambda <$ 0.75 nm 47% transported energy,
- INFRARED $\lambda > 0.75$ nm 46% transported energy.

Extraterrestrial radiation is the radiation that reaches the Earth from the Sun and has not yet suffered atmospheric attenuation. This radiation is subject to a geometric attenuation (squared proportionally to the distance), so that on the outside of the Earth's atmosphere, its value is $1.73 \cdot 10^{14}$ kW or, 1.353 kW/m^2, as the value of the solar constant, G_{sc}.

There are two sources of variation of the extraterrestrial solar radiation that must be considered (Duffie & Beckman, 2013). The inherent variation is the radiation emitted by the sun. It represents a very small value compared with atmospheric variations, and because of that, the energy emitted by the sun can be considered constant for engineering applications.

The Earth-Sun distance variation should also be taken into account to produce a variation of the flow of radiation in the range of ±3%. The dependence of the extraterrestrial radiation on the day of the year is given by Eq. (2.1).

$$G_{on} = G_{SC} \cdot \left(1 + 0.033 \cdot \cos \frac{360 \cdot n}{365}\right) \tag{2.1}$$

where n is the number of the day of the year, and G_{SC} is the solar constant earlier mentioned, with the value of 1.353 kW/m^2.

Through the atmospheric layer, the radiation is released and absorbed, even reflected by molecules suspended in it, as for example the water vapor condensed in clouds.

Some quantity of solar radiation will not find this obstacle. The types of radiation are described below according to their origin and scope:

Direct radiation (also referred to as beam radiation) is the solar radiation received at the Earth's surface without having undergone any change of direction in its path.

Diffuse radiation is the component of solar radiation received at the Earth's surface after the dispersion processes (reflection and dissemination) in the atmosphere.

Albedo radiation: is the component of solar radiation reflected from the surface.

The total solar radiation is the sum of direct, diffuse and albedo radiation.

It is possible to affirm that the incidental entire radiation over the Earth´s surface will be subject to variations, some predictable (daily and seasonal) and some unpredictable (the weather, particularly water vapor condensed in the clouds).

Therefore, as shown in Fig. 2.1, the spectral distribution of solar radiation at the sea level is modified with reference to the extraterrestrial. These variations are a problem for the exploitation of solar thermal energy, which can be mitigated with mechanisms of energy storage.

It should be stressed that the level of solar radiation that reaches the Earth´s surface is relatively moderate and even very low, as for industrial applications. It involves high costs and technology to take advantage of this energy. In situations where the required energy flows are not very high, it is possible to use diffuse radiation, which has the advantage of not requiring any kind of movement of the solar receptors to track the sun throughout the day. On the other hand, if energy applications require higher values of solar radiation, it is possible to concentrate this energy, but only with the direct radiation, which restricts the location of these applications to the locations of large amount of sunlight.

To estimate the production of heat or electricity, a reliable forecast of solar radiation is needed. This forecast is taken two or three days before the generation day and it lets us obtain the best thermal or electrical load production with enough anticipation.

To obtain a good forecast of solar radiation on the Earth's surface, we ought to consider the solar elevation (solar altitude above the horizon), the cloudiness produced by pollution and radiation absorption gases. Some statistical models, such as the Monte Carlo Method, are considered.

For standard location, the main radiation parameters referred to area unit are:
- daily irradiance of solar capitation area kWh/m^2,
- total heat over solar capitation area kWh/m^2,
- thermal efficiency peak (%) and daily peak (%),
- equivalent full load production hours.

Fig. 2.2 shows the monthly Direct Normal Irradiance (DNI) (kWh/m^2) and the sum of DNI for annual solar model in a specific location (South of Spain).

The studies of radiation are based on historical data obtained from public databases [WEB-2] of direct normal radiation through satellite (a minimum of 15 years) in periods of 10 minutes, with the clockwise angle and solar elevation angle.

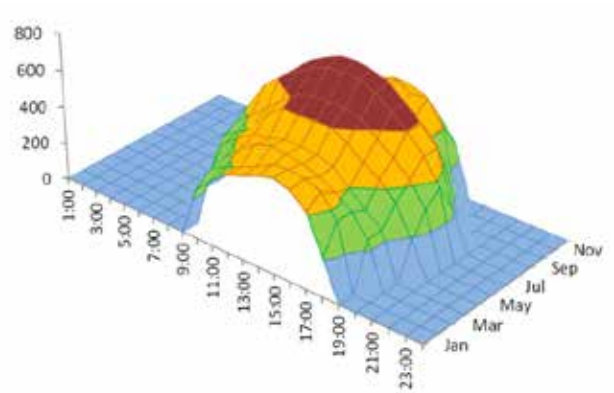

Fig. 2.2. Direct Normal Irradiance in a standard year solar model (Source: own elaboration)

The DNI for a standard clear day in this model is shown in Fig. 2.3 where we can see that solar to electric efficiency peak is lower than 25% (annual efficiency is about 14.7%).

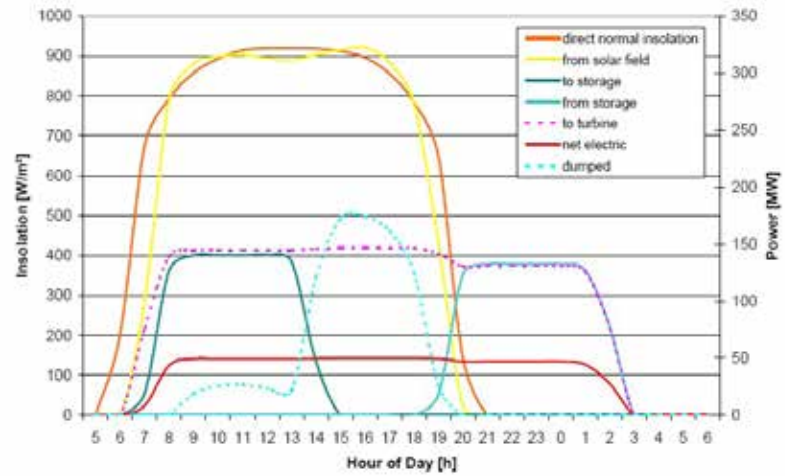

Fig. 2.3. Standard production in cloudless day model (Source: own elaboration)

For this application, short time forecast with meteorological details is usually the necessary tool for economical quantification. The tool named "*Simple Spectral Model for Direct and Diffuse Irradiance on Horizontal and Tilted Planes at the Earth's Surface for Cloudless Atmospheres*" (Turchi, 2010), developed by the National Renewable Energy Laboratory NREL, USA, makes predictions based on 10 years' data and implementation of algorithms with hourly precision for Direct Normal Radiation, Spectral Irradiance and total transmitted energy forecast.

With this tool, we are going to consider power vector obtained from estimated solar radiation as: $\Omega_t = \left\{EPw_t^1, EPw_t^2, ..., EPw_t^N\right\}$

With the considered probability vector $\rho = \left\{\rho_t^1, \rho_t^2, ..., \rho_t^N\right\} = \left\{1,1,...1\right\}$, the expected direct normal radiation $W_{DNI}(t)$, can be equalized to $R_{DNI}(t)$ in t period. The representation of complete radiation is as follows (Fig. 2.4 and 2.5):

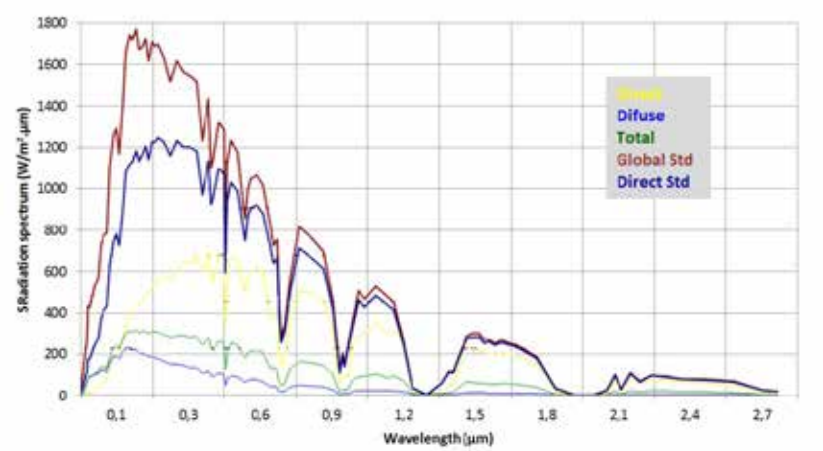

Fig. 2.4. Hourly solar radiation by specified spectrum (Source: Martínez-Val, 2004)

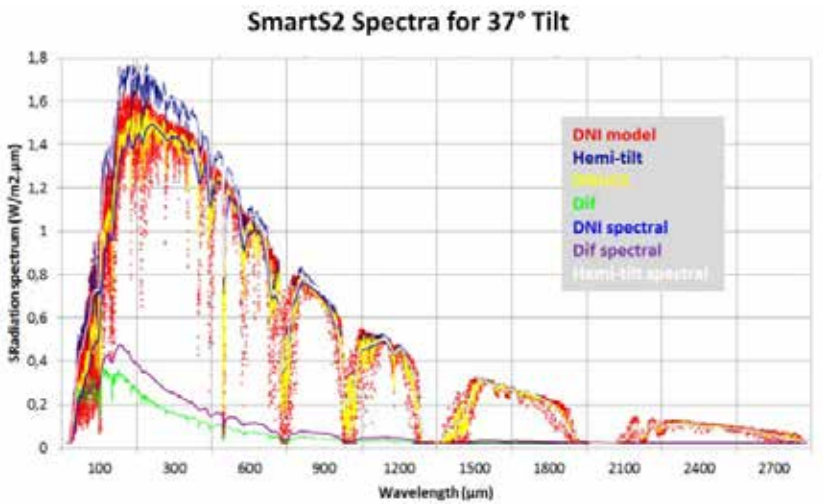

Fig. 2.5. Annual radiation for spectrum values (Source: Martínez-Val, 2004)

Total annual solar radiation on the surface of the Earth is estimated to be about 7500 times higher than the annual consumption of primary energy in the world

(Thirugnanasambandam et al., 2010). Trends in new investments in solar systems sector show increase, although once – in 2013, 18.5% a downfall was observed (Fig. 2.6). Taking into account utility-scale and small-scale, solar systems were by far the largest sector in capacity world investment. Until 2014, the developed economies (with Germany, Italy, Japan as leaders) dominated, while in 2015 a striking change happened and the gap in solar investment between the developed and developing countries (mostly because of China's and India's contribution) went down (80.8 versus 80.2 billion USD) (Frankfurt School-UNEP Collaborating Centre, 2016).

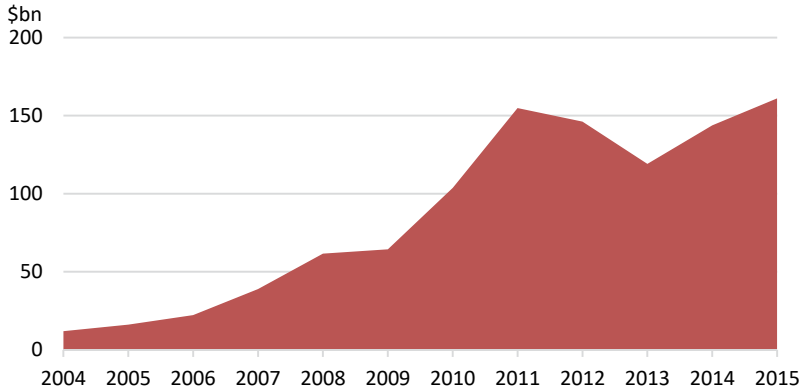

Fig. 2.6. New investment in solar sector in billions USD (Source: own elaboration based on Frankfurt School-UNEP Collaborating Centre, 2016)

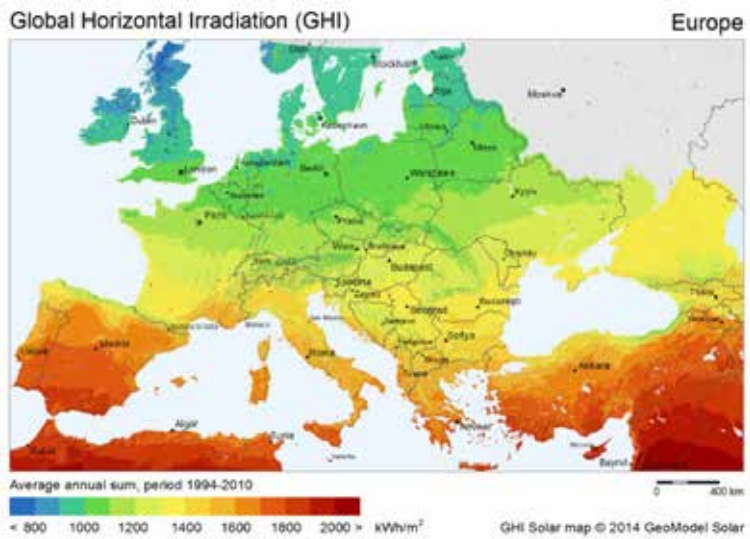

Fig. 2.7. Global Horizontal Irradiation in EU countries (Source WEB-2)

Development of solar systems depends on many factors including local climatic conditions, national policy, financial support, environmental consciousness etc. In Europe a significant diversity in global horizontal irradiation between countries can be observed (Fig. 2.7).

2.2. Solar collectors for thermal applications

2.2.1. Characteristic parameters for the thermal use of solar radiation

The heat transmission phenomenon for radiation is the main process of conversion of the solar energy to thermal energy. This involves the thermal energy from the Sun, as well as the transfer of heat into the solar collector by conduction and convection.

All materials and components emit electromagnetic radiation due to their own temperature, and are characterized through the intensity of radiation, I_e which is the rate of emission of radiant energy in a specific direction, per unit of area of the emitting surface normal to this direction and per unit of solid angle on this direction as shown in Eq. (2.2) (Siegel & Howell, 1992).

$$I_e(\theta,\phi) = \frac{dq}{dA_1 \cdot \cos\theta \cdot d\omega}\left(\frac{W}{m^2 \cdot sr}\right) \tag{2.2}$$

From this definition, there arise two concepts that are frequently used in solar energy, the emissive power of a specific surface *E*, and the irradiation *G*. The emissive power is defined as the speed of emission of energy per unit of surface [W/m^2].

In the case of a diffuse transmitter, the emissive total power, i.e. without preferred directions, adopts Eq. (2.3).

$$E = \pi \cdot I_e \tag{2.3}$$

where I_e is the total intensity [W/(m^2·sr)] of the emitted radiation. The emissivity is the parameter to characterize the emissive power. The emissivity, referred to as an ideal surface, is characterized by emitting more radiation in a given temperature. The emissivity of a black body supports a simple analytic expression, the Stefan-Boltzmann law, as shown in Eq. (2.4).

$$E_b = \sigma \cdot T^4 \left(W / m^2\right) \tag{2.4}$$

Where σ is the Stefan-Boltzmann constant, with the value of $5.67 \cdot 10^{-8}$W/m^2·K^4. The emissivity of a real surface is given by Eq. (2.5).

$$\varepsilon(T) = \frac{E(T)}{E_b(T)} = \frac{E(T)}{\sigma \cdot T^4} \tag{2.5}$$

On the other side, the irradiation G is the incidence of radiant energy per surface unit (W/m^2). G is the sum of emissions and reflections from other surfaces including the incident radiation from all directions. The total radiation, considering diffuse radiation, is given by Eq. (2.6).

$$G = \pi \cdot I_i \tag{2.6}$$

In global sense, the incident radiation can be reflected, absorbed or transmitted by the surface of considered material, as shown in Eq. (2.7).

$$G = G_{abs} + G_{ref} + G_{tr} \tag{2.7}$$

The determination of these three components depends on the conditions of the surface, the wavelength of the radiation and the composition of the material considered. Instead of working with the absolute values of these variables, it is preferred to handle proportions referred to the total value. Thus, to consider the absorbed radiation one should apply absorptivity, reflectivity to the amount reflected and transmissivity for the amount transmitted.

Absorptivity determines the fraction of radiation absorbed by a specific surface; the reflectivity is the fraction of radiation reflected by the surface; and the transmissivity is the fraction of radiation that is transmitted through the medium (Duffie & Beckman, 2013). These definitions are reflected in Eq. (2.8).

$$\alpha = \frac{G_{abs}}{G} \qquad \rho = \frac{G_{ref}}{G} \qquad \tau = \frac{G_{tr}}{G} \tag{2.8}$$

The black body, in addition to being the largest emitter for a given temperature, is characterized by the absorption of all of the incident radiation, regardless of the wavelength and the direction of such radiation, as expressed in Eq. (2.9).

$$\alpha = 1 \quad \text{or} \quad \rho \approx\sim 0 \tag{2.9}$$

Once these concepts of heat transfer by radiation have been introduced, it is necessary to perform a simple calculation to see what the maximum temperature or radiant equilibrium temperature is, T*, which can be achieved in a basic solar collector (Chapman, 1984). For this situation, a flat surface solar collector without solar concentration is considered. The total amount of absorbed energy per time and surface units is given by Eq. (2.10).

$$S = \alpha_c \cdot G_b \cdot \cos\theta_c \tag{2.10}$$

Where G_b is the direct irradiation from the Sun, α_c is the solar collector absorptivity, and θ_c is the incidence angle of the solar collector considering its angle of inclination. According to Eq. (2.5), the total amount of emitted energy from the collector surface per time and surface unit is given by Eq. (2.11).

$$E(T) = \varepsilon_c \cdot \sigma \cdot T^4 \tag{2.11}$$

Assuming, as a simplistic hypothesis, that the solar collector surface may only cool down by its own temperature radiation emission, the temperature T* is given by Eq. (2.12).

$$\varepsilon_c \cdot \sigma \cdot T^{*4} = \alpha_c \cdot G_b \cdot \cos\theta_c \quad \Rightarrow \quad T^* = \left(\frac{\alpha_c}{\varepsilon_c} \cdot \frac{G_b \cdot \cos\theta_c}{\sigma} \right)^{1/4} \tag{2.12}$$

This is the maximum temperature that a flat solar collector without concentration could reach. To increase the value of T*, it is necessary to use materials with a coefficient (α_c/ε_c) higher than one. These kinds of materials are good absorbers in the visible spectrum but not good absorbers in the thermal infrared spectrum. The second way to increase the value of T* is the utilization of solar concentration mainly by the direct irradiation (and small fraction of diffuse radiation). This solar concentration can be made by reflection (mirrors) or refraction (lenses). For photovoltaic applications, the refraction is more usual than reflection. For thermal applications, the reflection is the most frequent solution to concentrate the solar resource (Burlafinger et al., 2015).

2.2.2. Solar thermal technology

The solar energy collection (mainly in infrared spectrum) and its thermal exploitation by transmission fluid, has three usual active procedures considering the fluid temperature:

LOW TEMPERATURE (<90°C),

MEDIUM TEMPERATURE (<300°C),

HIGH TEMPERATURE (<800°C).

For low temperature heating, the application area for solar thermal energy extends from simply heating water to the so-called combi-systems, which can also be used for room heating, right through to solar thermal cooling and process heating systems. The first two types are used primarily in residential buildings.

The solar collectors without concentration are designed for applications with low temperature demand of energy, around 100°C or even 130°C for vacuum tube

collectors. They use both the direct radiation and the diffuse one and do not need a solar tracking.

The low temperature solar thermal systems operate with air conditioning systems and hot water. These systems have extended usage for domestic and industry direct use. This kind of system has a low cost of implementation, and average maintenance cost, and is usually integrated with conventional systems.

This kind of systems can be designed considering the solar resource to elevate the water temperature to higher limits or even to heat water to standard temperature but managing bigger volume of water to be heated (López-Cózar, 2006). This application can be extended to household and community buildings or even to heating swimming pools with the general scheme shown in Fig. 2.8.

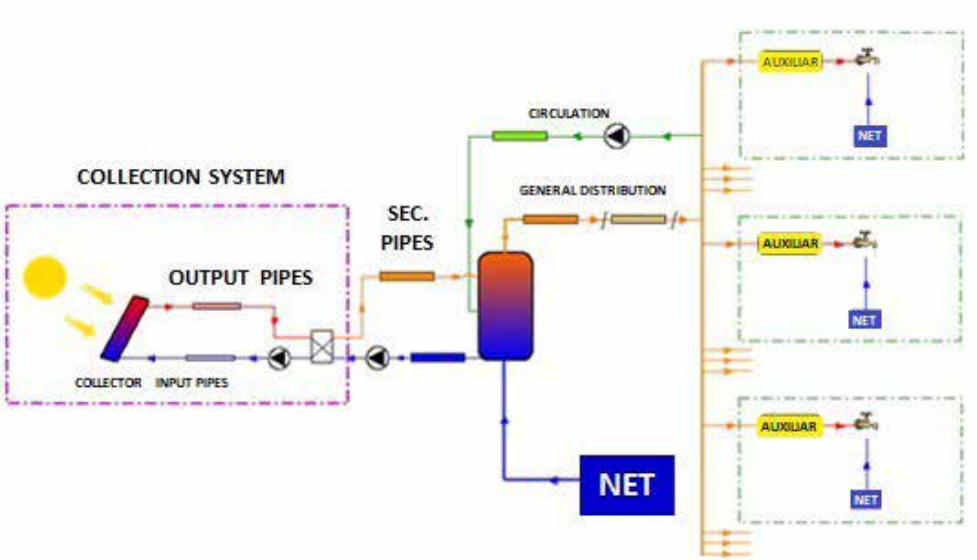

Fig. 2.8. High-volume water heating solar systems for household application (Source: own elaboration)

The two main types of solar thermal collectors used for domestic hot water are flat-plate and tube collectors (Fig. 2.9). The unglazed collectors are used for poor heating requirements, e.g. pool heating, while other collector types, such as air and ceramic collectors are used sporadically (Mahmut et al., 2015, Jebasingh et al., 2016). Table 2.1 shows the advantages, disadvantages and applications of these main collector types.

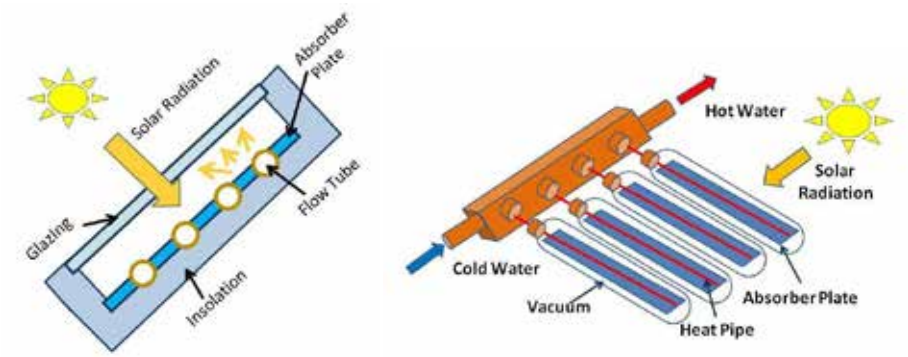

Fig. 2.9. Flat plate and tube collector schemas (Source: own elaboration)

Table 2.1. Characteristics of main collector types (Source: own elaboration)

	Advantages	Disadvantages	Application
Unglazed Collector	low cost	a lot of heat losses	pool heating
Flat Plate Collector	good cost-efficiency ratio	no high temperature	hot water 90% of the market
Tube Collector	– high efficiency – smaller space	high cost	– high temperature – low radiation – very popular in Northern Europe

2.2.3. Trends in the collectors market development

In Europe in 2013 most of newly installed collectors were dedicated to domestic hot water (DHW) systems for single family houses (68%). Large DHW systems work for multi-family houses and public buildings. Trends in the solar energy market for selected European countries are shown in Figs. 2.10, 2.11 and 2.12. The highest installed capacity in operation since 2004 has been observed in Germany, Greece and Austria. The number of newly installed area of glazed collectors was also significantly high in Germany, however it has decreased in the last three years. In all countries except Denmark reduction in annual installed area has been observed.

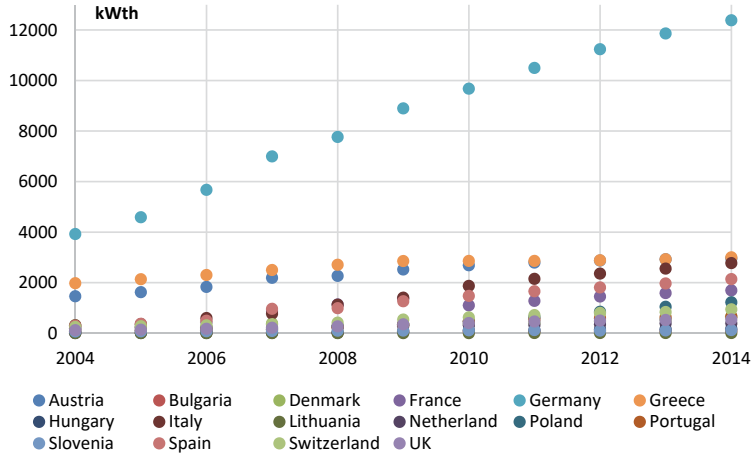

Fig. 2.10. Cumulative installed capacity in operation (kWth) (Source: own elaboration based on Matthner et al., 2015)

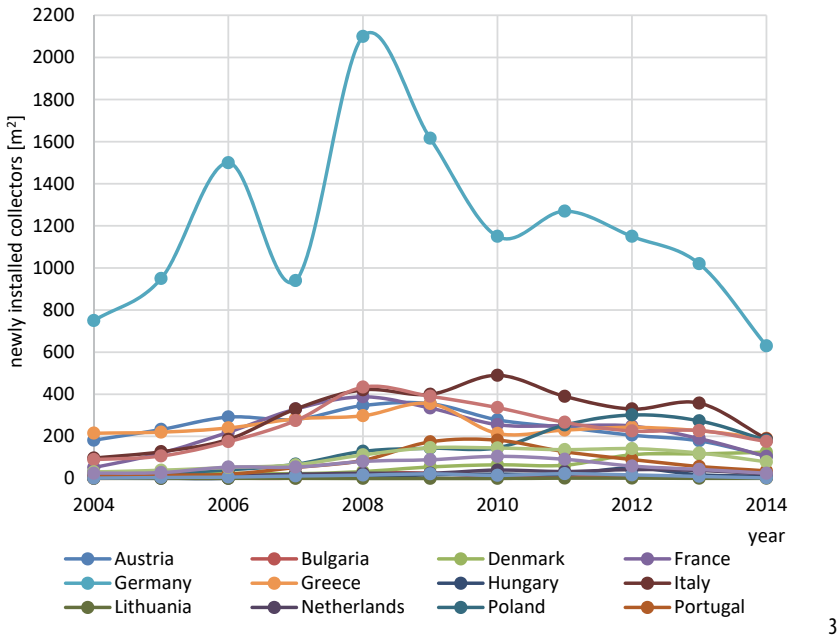

Fig. 2.11. Changes in newly installed glazed collectors per m² (Source: own elaboration based on Matthner et al., 2015)

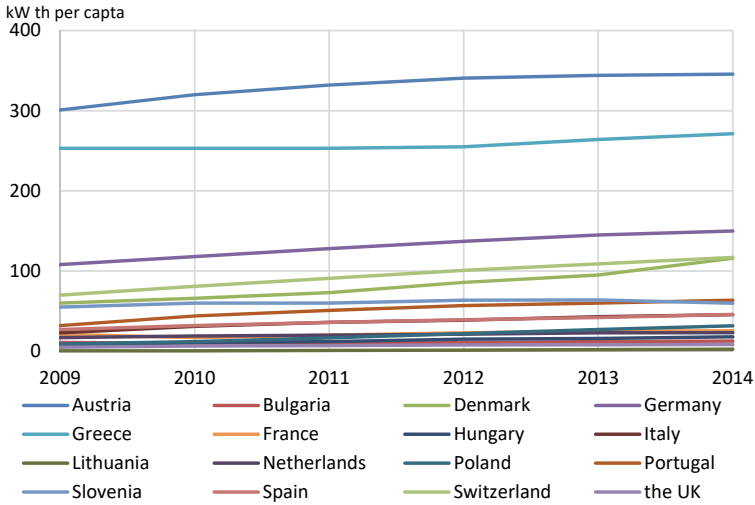

Fig. 2.12. Changes in newly installed kWth per 1000 habitants (Source: own elaboration based on Matthner et al., 2015)

Taking into account newly installed power per 1000 citizens – the best factor is obtained in Austria and Greece, about 3 times higher than in Germany. The lowest values were estimated in Lithuania (2.5 kWth per 1000 citizens) and the UK (8.4 kWth per 1000 citizens). Values for most countries were in the range of 23-63.6 kWth per 1000 citizens. In 2014 plate collectors were a huge part of the installed devices (Fig. 2.13). In some countries, for instance France or Denmark, they were the only ones in contrast to Lithuania or Hungary were vacuum tube collectors were more popular.

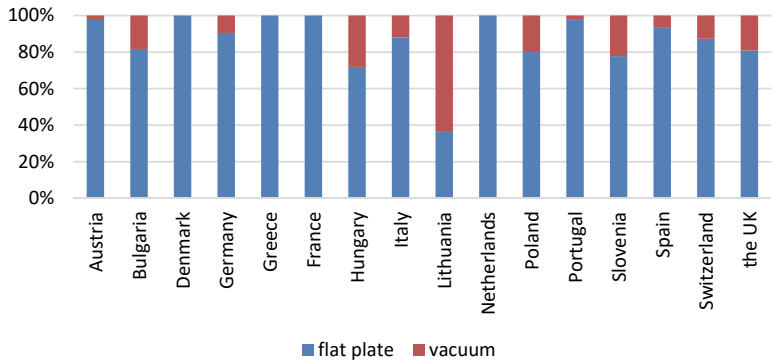

Fig. 2.13. Changes in newly installed capacity per 1000 collectors (Source: own elaboration based on WEB-3)

2.3. Simulation of the operation of a domestic hot water heating system supported by solar collectors

Issues related to computer simulation of thermal solar systems are very popular among both scientists and designers. Thanks to these techniques, we can estimate the parameters of solar systems during their operation and optimize them with low cost and great accuracy. Such computer-aided design of solar systems will lead to achieving their highest energy efficiency.

2.3.1. Efficiency of solar collectors

Duffie & Beckman (2013) developed a model that has been adopted as a standard for calculating the thermal characteristics of solar collectors in both flat and tubular designs. The efficiency of a solar collector h_{SC} is the most important parameter of its thermal performance. It can be defined as the ratio of the useful energy gain q_U at a certain time period to the solar energy incident on collector surface A_{SC} over the same period:

$$\eta_{SC} = \frac{\int q_U dt}{A_{SC} \int I_{SOL} dt}. \tag{2.13}$$

The instantaneous efficiency η_{SC} related to the gross area A_{GA} assuming steady state conditions, can be calculated as:

$$\eta_{SC} = \frac{q_U}{A_{SC} I_{SOL}}. \tag{2.14}$$

Energy balance on a solar collector is shown in Fig. 2.14. Part of the solar radiation I_{SOL} incident on the collector is reflected and is lost by conduction and radiation. The amount of heat loss depends primarily on the structure of the device.

The efficiency of the solar collector with double glazing, as a function of optical properties of glazing and absorber plate and environmental conditions, shows the following relation (EnergyPlus, 2016):

$$\eta_{SC} = \tau_{G1}\tau_{G2}\alpha_{ABS} - \frac{T_{ABS}^4 - T_{G2}^4}{R_{RAD}} - \frac{T_{ABS} - T_{G2}}{R_{CONV}} - \frac{T_{ABS} - T_{AMB}}{R_{COND}}, \tag{2.15}$$

where:

τ_{G1} – transmittance of the first glazing (–),
τ_{G2} – transmittance of the second glazing (–),

α_{ABS} – absorber plate emissivity (–),
T_{ABS} – temperature of the absorber surface (°C),
T_{G2} – temperature of the second glazing (°C),
T_{AMB} – ambient air temperature (°C),
R_{RAD} – heat transfer resistance by radiation from absorber to inside glazing (1/°C^4),
R_{CONV} – heat transfer resistance by free convection from absorber to inside glazing (1/°C),
R_{COND} – heat transfer resistance by conduction from absorber to ambient air (1/°C).

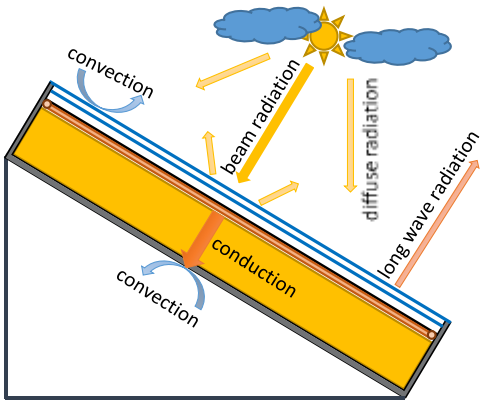

Fig. 2.14. Energy balance of gains and losses for a thermal collector (Source: own elaboration)

In practice, the above equation is approximated to the following simplified form:

$$\eta_{SC} = f_R(\alpha\tau) - f_R U_C \frac{T_{IN} - T_{AMB}}{I_{SOL}}, \tag{2.16}$$

where:
f_R – correction factor determined by the experiment (–),
$(\alpha\tau)$ – optical characteristics of the collector (–),
U_C – overall heat loss coefficient of the collector (W/(m^{2}K)),
T_{IN} – inlet temperature of the working fluid (°C),

or in simplified notation:

$$\eta_{SC} = \eta_{SC,0} - a_1 \frac{T_{IN} - T_{AMB}}{I_{SOL}}, \tag{2.17}$$

where:
$\eta_{SC,0}$ – zero-loss collector efficiency (–),
a_1 – heat loss coefficient (W/(m^{2}K)).

In order to increase the accuracy of determining the instantaneous efficiency, the following formula (ISO, 2013) was proposed, based on the second-order curve which is mostly used in the modelling of solar systems:

$$\eta_{SC} = \eta_{SC,0} + a_1 \frac{T_{IN} - T_{AMB}}{I_{SOL}} + a_2 \frac{\left(T_{IN} - T_{AMB}\right)^2}{I_{SOL}}, \tag{2.18}$$

where a_2 – temperature dependence of the heat loss coefficient (W/(m²K)).

The values of all the coefficients in the above equation can be found on the website of the Solar Rating & Certification Corporation (ICC-SRCC) arranged by manufacturers of solar collectors.

The transmittance properties of the collector glazing depend on the angle of incidence of solar radiation. In order to take into account the impact of this phenomenon on the characteristic of a collector, there has been proposed an incident angle modifier coefficient $K_{\tau\alpha}$:

$$K_{\tau\alpha} = 1 + b_0\left(\frac{1}{\cos\theta} - 1\right) + b_1\left(\frac{1}{\cos\theta} - 1\right)^2, \tag{2.19}$$

where:

b_0, b_1 – incident angle modifier coefficients (–),
θ – angle of incidence of solar radiation (deg).

The values of both coefficients can be found in certification documents prepared by the ICC-SRCC.

2.3.2. Software used for simulation of solar systems

The most advanced and popular software used for computer simulation of building energy consumption and modelling of solar collector systems are the following tools: ESP-r, DesignBuilder, OpenStudio, EnergyPlus, SUNREL, TRACE 700, TRANSOL – Solar Thermal Energy, HVACSIM+, HEED Home Energy Efficient Design, RETScreen, Polysun, and TRNSYS.

This book provides an example of a year-round modelling of the solar collector system using the verified and fully validated tool – EnergyPlus.

In EnergyPlus, solar radiation is calculated based on the anisotropic (non-uniform) radiance distribution of the sky. In this model the total radiation I_{SOL} is a combination of the direct (beam) I_{DIR}, diffuse I_{DIF}, and reflected I_{REF} solar radiation. These values with a one-hour time step are taken directly from the weather data (WEB-4). Weather

information for a typical meteorological year is now available for more than 2100 locations all over the world.

One of the parameters affecting the efficiency of solar collectors is their shading. In EnergyPlus, two procedures are used for shadowing calculations: Groth and Lokmanhekim (1969) coordinate transformation method and Walton (1983) shadow overlap method. These procedures were adopted from other simulation tools: BLAST and TARP.

EnergyPlus allows to simulate the operation of the entire system consisting of solar collectors, storage tanks, auxiliary heaters and automatic control valves, as shown in Fig. 2.15.

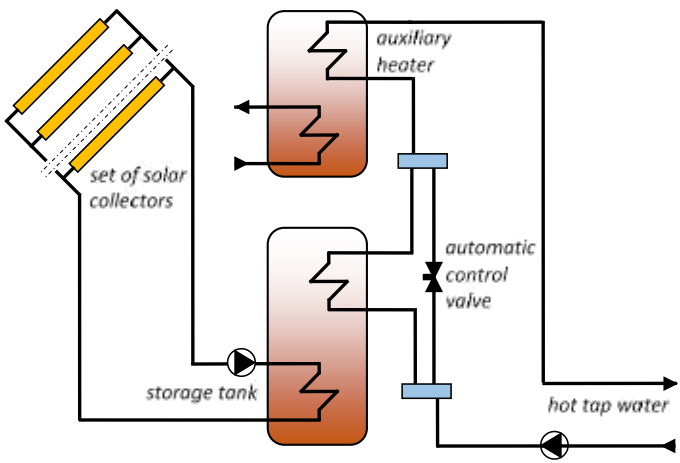

Fig. 2.15. Schematic diagram of device connection system used in simulations (Source: own elaboration)

2.3.3. Characteristics of data used for simulation

This chapter describes practical aspects of modelling solar collectors that support the domestic hot water (DHW) system. The stages of this complex simulation process are illustrated with the example of High School No. 8 building, located in Bialystok (Fig. 2.16). This type of facility has been selected for the analysis because it is characterized by reduced demand for hot water in summer. In the recent time, solar collectors are often installed in school buildings. Therefore, the following analysis will show the effectiveness of these devices during summer holidays, while the intensity of solar radiation is highest.

Fig. 2.16. View of the High School No. 8 building (Source: WEB-5)

The scope of necessary data which should be prepared is shown below. The interpretation of vast database of calculation results is discussed, too. As mentioned earlier, the EnergyPlus program was used to perform these simulations. However, methodology of the entire modelling process remains common to all such computer tools.

To compare the impact of different locations on the energy efficiency of solar collectors, two other locations: in Cordoba and Kaunas were also considered.

The data for the typical meteorological year for the Bialystok station (POL _ Bialystok.122950_IMGW), the Cordoba station (ESP_Cordoba.084100_ SWEC), and the Kaunas station (LTU_Kaunas.266290_IWEC) was taken into account in the simulations. Calculations were made for the whole year with a one-hour time step, because meteorological data was also prepared with the same time step.

The outdoor temperature (Fig. 2.17), direct solar radiation (Fig. 2.18), and diffuse solar radiation (Fig. 2.19) charts are presented in order to compare the climatic conditions of these three cities. The average monthly values of climatic parameters are shown on these graphs.

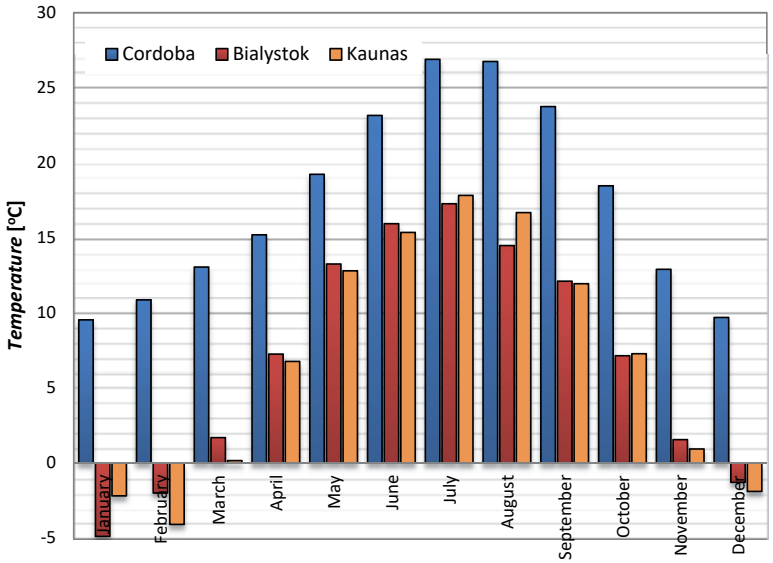

Fig. 2.17. Monthly average outdoor air dry-bulb temperature (Source: own elaboration)

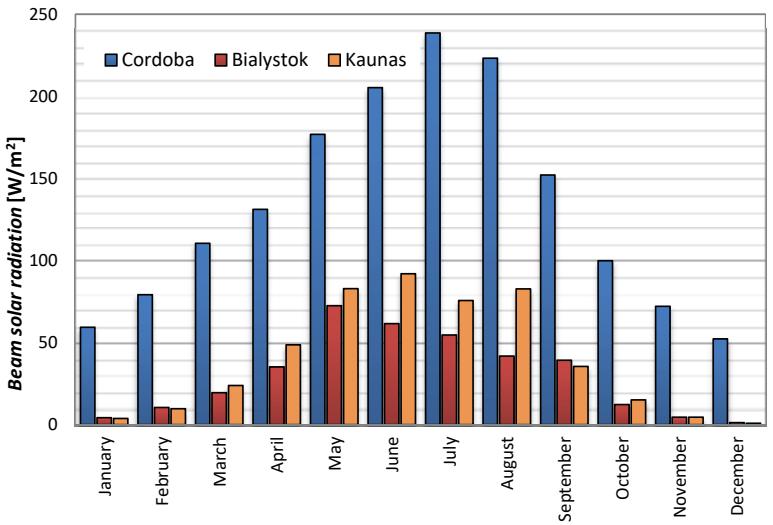

Fig. 2.18. Monthly average beam solar radiation rate per square metre falling on a horizontal surface (Source: own elaboration)

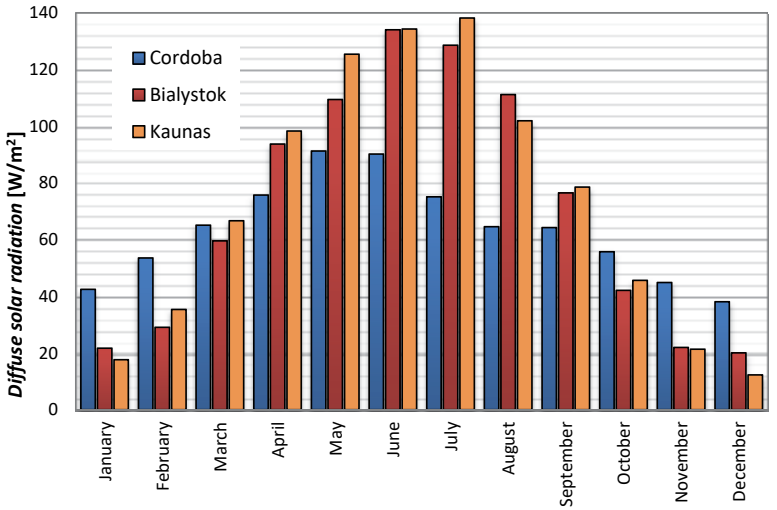

Fig. 2.19. Monthly average diffuse solar radiation rate per square metre falling on a horizontal surface (Source: own elaboration)

Based on the analysis of the graphs shown in Figs. 2.17, 2.18 and 2.19 it can be stated that the intensity of solar radiation and the temperature of outdoor air are similar in Bialystok and in Kaunas. Cordoba, on the other hand, is characterized by very high direct radiation and high external temperature compared to the other two locations. Certainly such meteorological conditions affect significantly the amount of energy generated by solar collectors.

Hot water demand in High School No. 8 was determined on the basis of energy consumption for the heating of cold water. This value was read from the heat meter. Consumption of domestic hot water in the form of average monthly values is shown in Fig. 2.20.

Energy consumption for heating of DHW depends directly on the cold water temperature T_C that feeds the system. Cold water parameters are calculated separately for each day based on the relationship given by Hendron et al. (2004). The value of T_C (Eq. 2.20) depends on outdoor air temperature and is a function of average annual outdoor air temperature $T_{AMB,A}$ and maximum difference in monthly average outdoor air temperature $\Delta T_{AMB,D}$.

$$T_C = (T_{AMB,A} + 6) + \text{ratio}\ (\Delta T_{AMB,D}/2)\ \sin[0.986(\text{day} - 15 - \text{lag}) - 90], \quad (2.20)$$

where:
ratio = $0.4 + 0.01(T_{AMB,A} - 44)$;
lag = $35 - (T_{AMB,A} - 44)$.

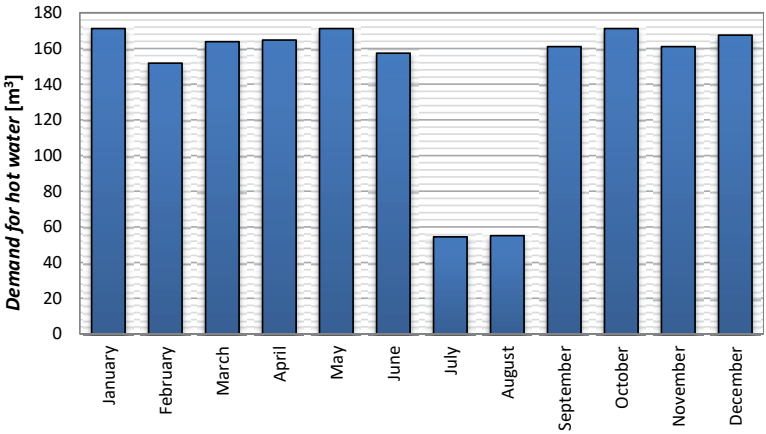

Fig. 2.20. Average monthly consumption of hot water (Source: own elaboration)

The temperature profile of the cold water for three analysed locations is presented in Table 2.2. The parameters used as input data for EnergyPlus software are as follows:

Table 2.2. Parameters for Bialystok, Cordoba and Kaunas (Source: based on the author's calculations)

	Bialystok	Cordoba	Kaunas
$T_{AMB,A}$	6.92	17.49	6.79
$\Delta_{TAMB,D}$	22.17	17.36	21.92

Table 2.2 clearly shows that, cold water temperature is almost the same for Bialystok and Kaunas, but definitely higher for Cordoba. The average annual value of T_C for Bialystok, Kaunas and Cordoba is 10.2°C; 10.1°C; 20.8°C, respectively. Therefore, we can calculate that heating the mains cold water to 50°C consumes about 26% less energy in Spanish cities compared to the cities located in Central and Eastern Europe.

The following main assumptions regarding the solar system were made:

- 30 solar collectors with the following parameters:
  - gross area: 2.05 m^2;
  - test flow rate: 0.0166667 l/s;
  - zero-loss collector efficiency: 0.784;
  - heat loss coefficient: –3.64 W/(m^2K);
  - temperature dependence of the heat loss coefficient: –0.00185 W/(m^2K^2);
  - incident angle modifier coefficients (b_0): –0,121;
  - incident angle modifier coefficients (b_1): 0.

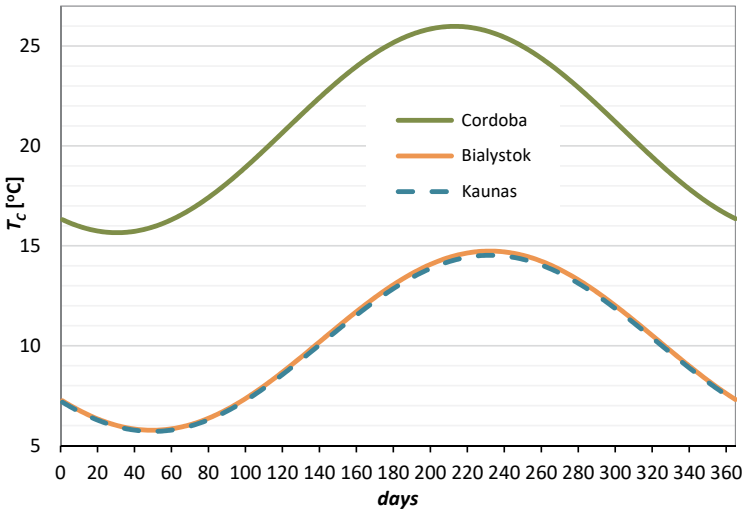

Fig. 2.21. The change in the cold water temperature during a typical meteorological year (Source: own elaboration)

- Storage tank with 4 m^3 capacity.
- Storage water temperature: 60°C.
- Hot water set-point temperature: 50°C.

2.3.4. Results of modelling the operation of the domestic hot water system supported by solar collectors

The calculations were performed for the entire period of one year (8,760 hours) with one-hour time step. Modeled object is shown in Fig. 2.22.

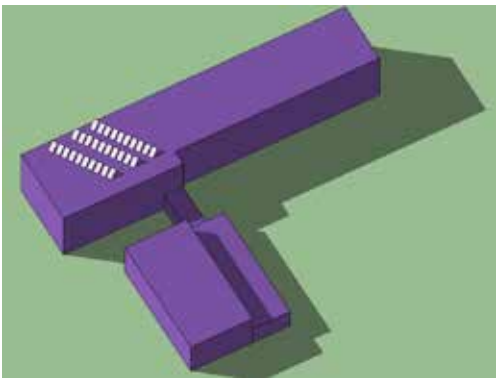

Fig. 2.22. EnergyPlus 3-D model of High School No. 8 building with solar collectors (Source: own elaboration)

The selected results of simulations are presented in the form of graphs. The most important element that an investor is interested in is the amount of useful energy produced by the solar collectors. Fig. 2.23 presents the energy gains according to the location of the solar system. The total amount of energy per year that we can get from 1 m^2 of collector gross area is 635.85 kWh for Cordoba and twice less for Bialystok – 335.25 kWh and Kaunas – 369.45 kWh. A very significant difference in useful energy between locations is observed in the winter months. From November to February the solar system located in Cordoba produced 13623 kWh of heat, while the other systems produced only 698 kWh (Bialystok) and 511 kWh (Kaunas) – about 20 times less. During the two summer months of July and August the situation is changing. This unexpected effect is primarily due to the low demand for DHW and the high temperature of cold water in Cordoba.

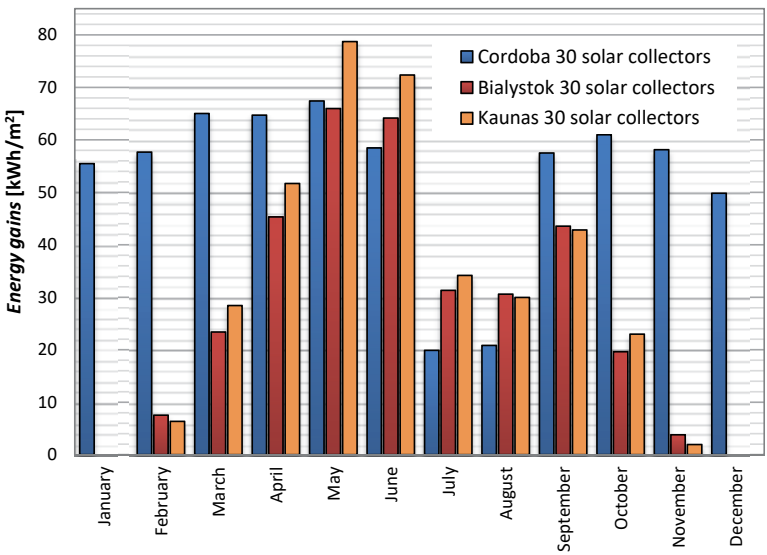

Fig. 2.23. Useful energy gained by the solar systems – average monthly values (Source: own elaboration)

Another important issue that is of most interest to the investor is the amount of energy that must be used for the preparation of DHW additionally. The diagram in Fig. 2.24 shows that in the case of Cordoba we have to provide additionally 20.8% energy coming from auxiliary heater, while in case of localization in Poland this value is up to 72% and in Lithuania – about 70%.

Another conclusion we can come up with after analysing the graph in Fig. 2.24 is the excessive number of solar panels in Cordoba. Such computer simulations can also be used to determine the optimum number of these devices.

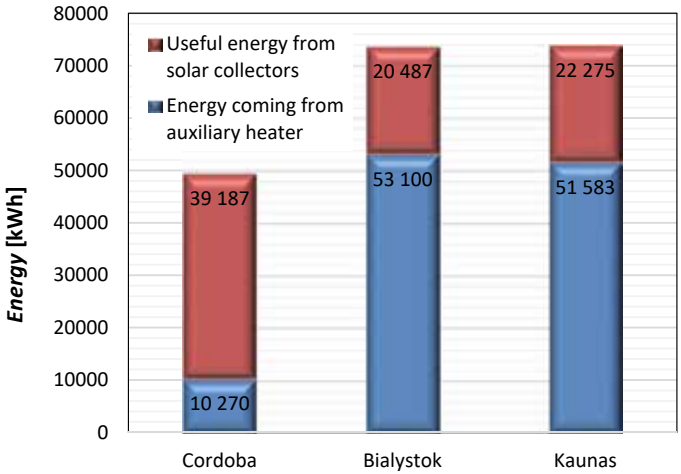

Fig. 2.24. Comparison of useful energy gained by 30 solar collectors and energy coming from auxiliary heaters for systems located in Cordoba, Bialystok and Kaunas (Source: own elaboration)

Therefore, additional series of calculations were carried out for 20 and 10 collectors for the location in the Spanish city. The results of simulations are shown in Fig. 2.25. As can be seen, the smaller number of solar collectors increases their energy efficiency. This is particularly evident during the summer months. The increase of useful energy (average value throughout the year) supplied by the 1 m^2 gross area of a collector is 22% while reducing their number to 20, and 54% by reducing their number to 10 panels. The next graph in Fig. 2.26 presents the comparison of useful energy and energy coming from auxiliary heaters for three solar collector systems located in Cordoba.

In order to determine the optimal number of solar panels we should obtain Solar Fraction (*SF*). This parameter is defined as the ratio of energy provided by solar collectors to the total energy required by the system. As shown in Fig. 2.27, the annual average of *SF* varies from 40% to 80% depending on the number of collectors for the irradiance conditions in Cordoba. When we assume that the solar system should be able to provide around 50% of total energy demand for water heating, it turns out that only 15 collectors will be suitable for this building.

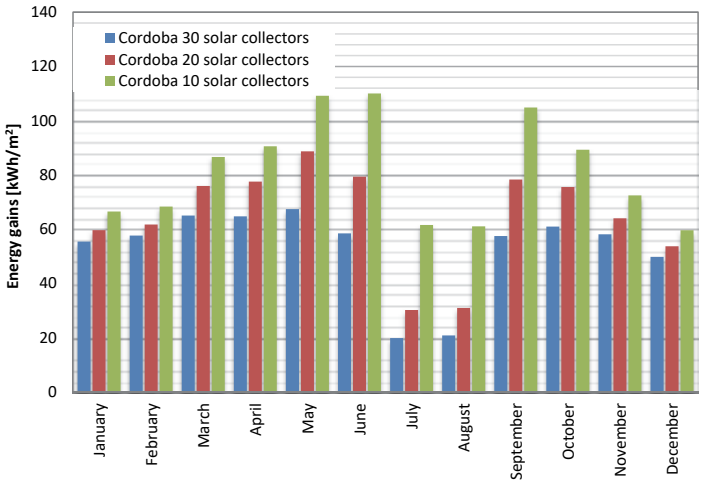

Fig. 2.25. Useful energy gained by 30, 20, and 10 solar collectors for the system located in Cordoba (Source: own elaboration)

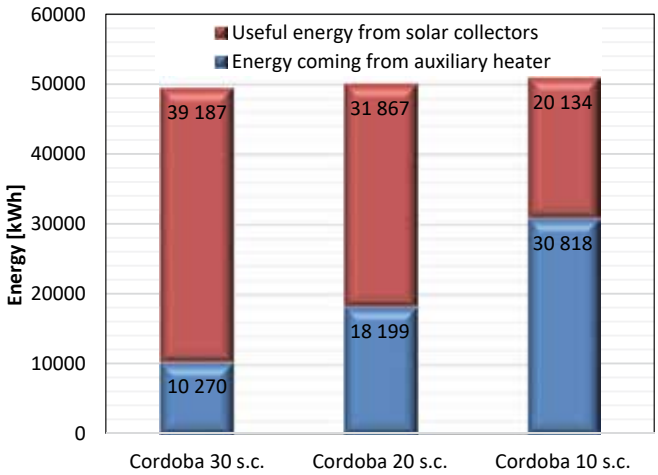

Fig. 2.26. Comparison of useful energy gained by 30, 20, and 10 solar collectors and energy coming from auxiliary heaters for the system located in Cordoba (Source: own elaboration)

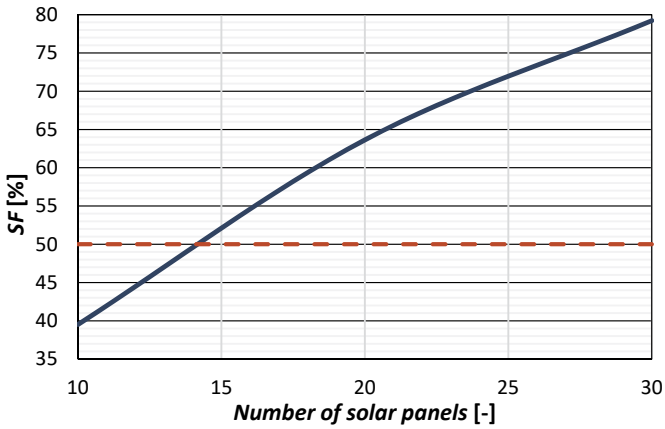

Fig. 2.27. Annual average *SF* value as a function of the number of solar panels (Source: own elaboration)

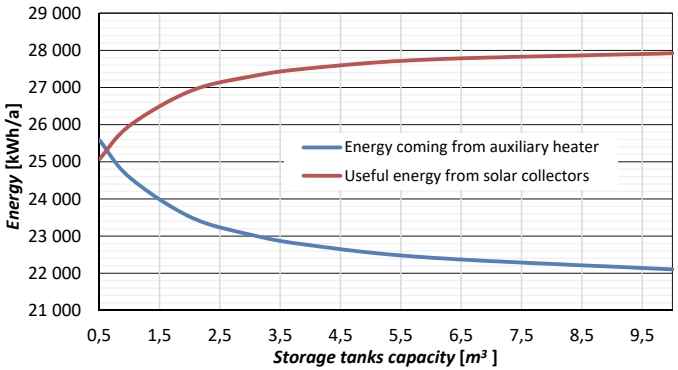

Fig. 2.28. Useful energy gained by solar collectors and energy coming from auxiliary heaters as a function of hot water storage tank capacity (Source: own elaboration)

Another advantage of using computer simulations is the ability to determine the optimum volume of the hot water storage tanks. For this purpose, seven series of calculations were made for 15 solar panels located in Cordoba, and the volume of storage tanks was assumed as follows: 0.5; 1; 2; 3; 4; 6; 10 m^3. By analysing the graphs in Fig. 2.28, it can be stated that the optimum volume of the hot water tanks is about 4 m^3. Increasing their volume above this value leads to only very small energy gains. It should be noted that increasing the capacity of the tanks is not only associated with higher investment costs but also with an increase in heat loss.

In conclusion, it must be stated that the use of computer simulation methods is a very effective tool and should be a common practice for a designer of medium- and large-scale solar water heating systems.

2.4. Concentrating solar thermal technologies

For medium and high temperatures, the capture of solar radiation is performed by concentrating solar thermal systems (STC) (García-Casals, 2001). The solar collection is made by a special type of heat exchanger that transforms the radiant energy from the sun into thermal energy. This type of exchange has variable energy flows, which is the main technical difficulty for management.

A solar collector has two main operational parts, a receiver and a concentration tube. The receiver is the element of the system where the radiation is absorbed and converted into another type of energy; it includes the absorber, fixed covers and the insulator. The concentration tube or optical system is the part of the collector which directs the radiation to the receiver. The opening of the concentrator is an open space through which the solar radiation enters the collector.

Taking into account the concentration of solar radiation, the reason or factor of concentration C is considered as the ratio between the opening area of the solar collector referred to the receptor area, as defined in Eq. (2.21) (Winter et al., 1990):

$$C = \frac{A_a}{A_r} \tag{2.21}$$

Considering the temperature of reception and the reason of final concentration of solar radiation, the systems of reception for generation of electricity are classified in Table 2.3, detailed in Fig. 2.29 and 2.30 and explained in the following paragraphs (Kalogirou, 2009):

Table 2.3. Classification of solar technologies (Source: own elaboration)

Collector type referred to its concentration factor and temperature					
No Concentration (C=1)			With Concentration (C>1)		
Non-glass collector	Flat surface collector	Advanced collectors	Parabolic trough	Solar tower	Parabolic dish
		Absorber with selective surface	C∈[30,90]	C∈[200,1000]	C∈[1000,5000]
		Vacuum tube collector			

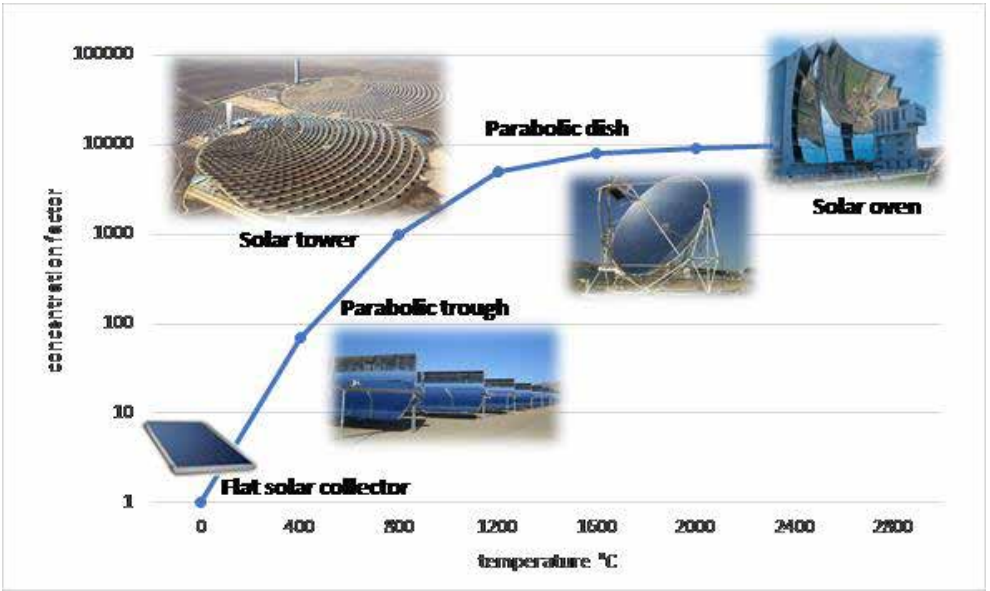

Fig. 2.29. Classification of solar collectors according to their temperature (Source: own elaboration based on García-Casals, 2001)

2.4.1. Parabolic Trough Reflector (PTR)

The parabolic trough reflector is a collection system formed by cylindrical mirrors whose cross section is a parabola, so that the solar radiation is concentrated in the focal centre in which the receiver (absorber tube) is placed. The parabolic trough can obtain concentration factors between 30 and 90. This system includes solar trackers of concentration on high efficiency heat piping by carrying synthetic oil, steam water or molten salt as an element of heat transfer. Its maximum working temperature is 550°C. PTRs are susceptible to work coupled with heat storage systems by heat exchanger (Antonelli et al., 2015).

2.4.2. Solar tower technology

The Solar tower is a collection system based on the concentration of radiation provided by mirrors, heliostat devices, distributed on a horizontal surface, and oriented to reflect solar radiation towards the receiver on top of the tower. The projection to the tower is almost 6000% of the radiation received by one collector. Its working temperature is above 600°C, with frequent intervals of temperatures reaching between 900°C and 1200°C. Tower technology can be combined with other thermal systems such as solar convection chimneys.

2.4.3. Solar dish

Parabolic dishes are mirrors with a paraboloid of revolving structure, which are monitored to always maintain their orientation toward the sun. The modular installation of high temperature parabolic troughs (600ºC) is susceptible to coupling in parallel for electricity generation. The generation of electricity is performed using individual Stirling generators. Its main application is the solar collection in irregular extensions or surfaces.

2.4.4. Linear concentrator Fresnel

It consists of a primary field of mirrors, an absorber tube and a secondary mirror. The primary field contains rows of flat mirrors that reflect the solar radiation to the absorber tube located several meters above the main field. Above the absorber tube a secondary mirror is located which concentrates the remaining sunlight in the linear absorber tube. This type of installation stands out for the simplicity of its construction and its low cost. Fresnel technology uses flat reflectors, simulating a curved mirror by variation of the adjustable angle of each individual row of mirrors, in relation to the absorber.

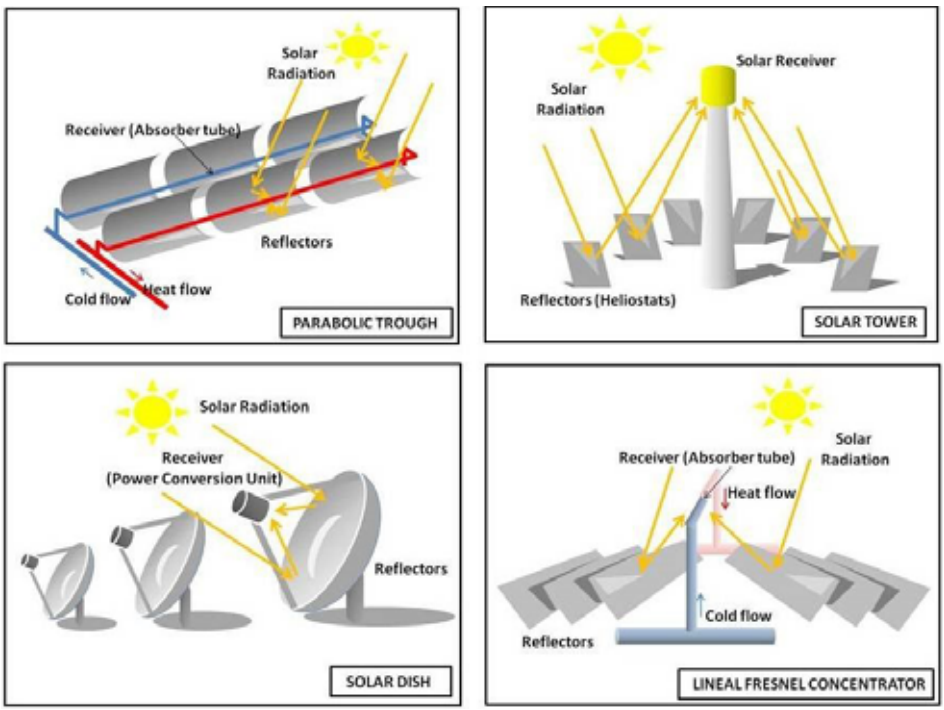

Fig. 2.30. Main concentrated solar technologies (Source: own elaboration)

Reflectors are constructed with normal glass mirrors and therefore their raw material is very cheap. The curved shape of the parabolic cylinder mirrors makes them 15% more efficient than the Fresnel mirrors, but the reduction of the construction costs compensates the reduction of efficiency.

With any of these four technologies it is possible to concentrate the solar irradiation, which can be considered approximately parallel and incident in a large area (concentrator) over a small one (the receiver). Therefore, the optimum geometry of the concentrator is a paraboloid of revolution with orientation toward the Sun movement. This geometry has the highest concentration values. Thus, parabolic cylinder systems allow to concentrate the solar radiation along an axis. In the central tower systems, the surface of the concentrator is discretized in a series of heliostats as a Fresnel concentrator, i.e. a parabolic reflector through small segments.

Medium and high temperature systems are not used for domestic applications but are desirable for certain industrial applications where large amounts of hot water are needed mainly for producing electricity by steam-driven turbines in solar power plants.

2.5. Electricity applications

2.5.1. Concentrated solar power plants

Concentrated solar power (CSP) plants, also called solar thermal power plants, are systems that collect and concentrate light from the sun to produce high temperature needed to generate electricity. CSP technologies are currently in medium to large-scale operation with a production of about 4.8 GW in 2016, and are mostly located in Spain and the USA (Fig. 2.31), although China has 20 pilot projects to produce 9.6 GW in 2020. Parabolic trough reflector (PTR) technology is responsible for 96.3% of total world thermal energy production and solar tower is in the second place as shown in Fig. 2.32.

All solar thermal power systems have solar energy collectors with two main components: *reflectors* (mirrors) that focus solar radiation onto a *receiver*. A heat-transfer fluid is heated and circulated in the receiver and used to produce steam. The steam is converted into mechanical energy in a steam-driven turbine, which produces electricity by a generator. Optionally, solar thermal power systems have a thermal energy storage or backup system to supply energy when the solar radiation is not strong enough.

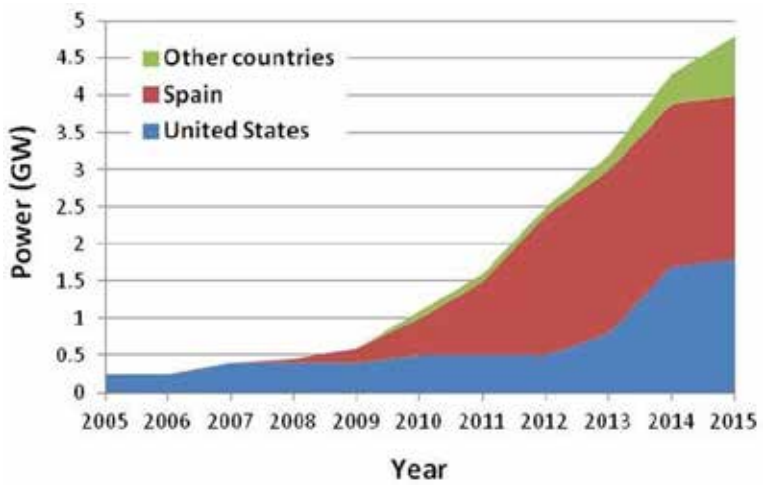

Fig. 2.31. Global Capacity of Concentrated Solar Thermal Power from 2005 to 2016 (Source: own elaboration based on REN21, 2017)

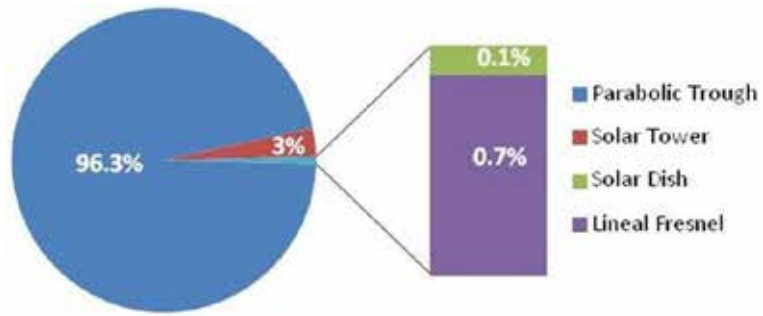

Fig. 2.32. Percentage of installed operational CSP power by technology (Source: own elaboration based on Zhang et al., 2013)

Fig. 2.33. Parabolic trough reflector plant "LA AFRICANA" in Cordoba (Source: photo by A. Rodero)

Parabolic trough reflector (PTR) plants (Fig. 2.33) use heat-transfer fluid (HTF) which, when circulating through the tube receiver, absorbs the radiant energy from the Sun in the form of thermal energy, and transports it to the thermal cycle. The type of heat transfer fluid used determines the range of operating temperatures and consequently the efficiency that can be obtained in the power cycle. Fig. 2.34 shows a schema of main parts of a typical PTR plant.

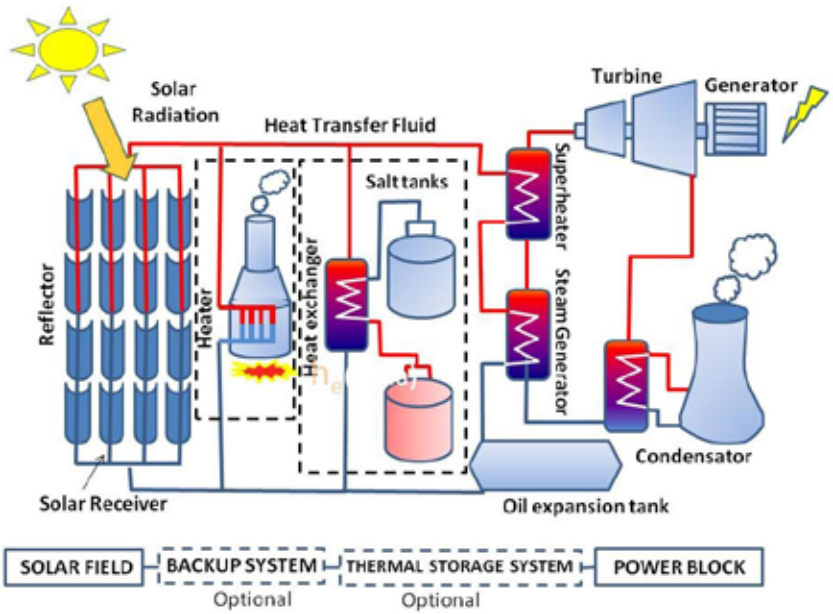

Fig. 2.34. Schema of a concentrated solar plant (Source: own elaboration)

The normal temperature range of HTF is between 150-500°C. Water can be used as HTF for temperatures below 150°C. For higher temperatures, the pressure in the pipes is so high that it makes the installation too expensive. Synthetic fluid is used when higher temperatures are needed.

Currently, synthetic aromatic oil based on benzene is used in commercial PTR plants. Main thermodynamic properties of this fluid are shown in Table 2.4. It is a fluid that turns to solid state below 12°C and flows with difficulty below 25°C. This means that it is important to avoid lowering the temperature. An additional heating system is necessary to ensure sufficiently high temperatures. This system can use traditional fossil fuel, e.g. natural gas that can supply additional energy when radiation is low.

HTF oil presents cracking problems in temperatures above 430ºC. Above this temperature, molecules are broken, producing other hydrocarbon species that modify the properties of HTF. There are two protection systems:

- A control system: to ensure a minimum flow so that the pipe temperature does not exceed that of cracking. Pumps used in PTR plants are Sulzer of 1MW or Novo Pignone of 2 MW working under pressure from 15 to 30 bar. Also some unneeded collectors can be unfocused to avoid overheating.
- A system of residue elimination (Ullaje system) to eliminate oxidation and cracking products from HTF. A 2% of oil is heated to the boiling point and subsequently cooled to separate these residues with different thermodynamic characteristics.

The density of HTF oil has a great dependence on temperature. This means you need an expansion tank to control the large volume changes.

Table 2.4. Thermodynamic characteristics of the HTF oil (Source: own elaboration based on WEB-6)

Thermodynamic parameters	Value
Melting temperature	12ºC
Cracking temperature	430ºC
Density	1060 kg/m^3 (25ºC) 690 kg/m^3 (393ºC)
Vapour pressure	10.6 bar (393ºC)
Specific heat	2300-2700 J/kg
Enthalpy	540 kJ/kg (293ºC) 800 kJ/kg (393ºC)
Viscosity	0.12 mPa s (393ºC) Very high below 25ºC

Thermal energy storage and backup system

As mentioned above, in order to improve its competitiveness in relation to conventional systems with stable power supply, the PTR plant can be enhanced with a thermal storage system or/and a backup system used in case of low solar radiation.

Thermal energy storage systems (TES). The problem with excess heat in a solar plant is solved by defocusing some unneeded collectors to avoid overheating of HTF. TES allows to store excess heat collected in the solar field. This excess heat is sent to a heat exchanger and warms the heat transfer fluid (HTF) which passes to the energy storage tank. When needed, the heat from the hot tank can be returned to the HTF and sent to the steam generator (Fig. 2.35).

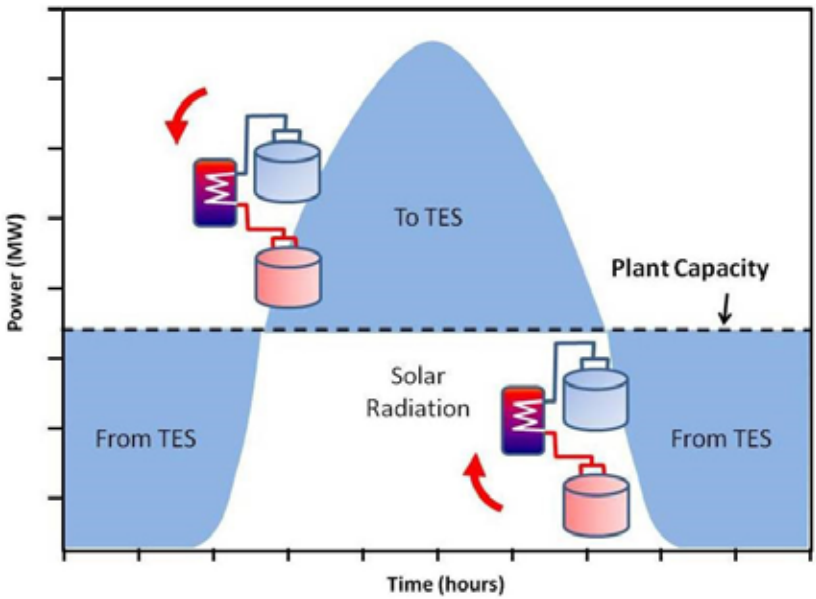

Fig. 2.35. Power contribution of TES in a PTR plant (Source: own elaboration)

The characteristic features of the energy storage materials are high density, low vapour pressure, moderate specific heat, low chemical reactivity and low cost (Zhang et al., 2013). Currently, molten salt is most often used but other systems have been tested with sensible and latent heat storage:

- The storage of sensible heat with synthetic oil (or own HTF). It is a more expensive system because it needs a bigger storage tank and also it is very dangerous because of its flammability.
- The storage of sensible heat in solid concrete. HTF flows by holes made in the concrete, heating it. This energy is recovered when needed.
- The storage of latent heat by means of melting solid salt. The advantage of the system is that doesn't need to pump salt and uses less salt for the same energy storage. This technology is currently under development.

Pure molten salt tends to be expensive, so a mixture of 60% sodium nitrate ($NaNO_3$) and 40% potassium nitrate (KNO_3) is used. This material is a stable mixture with low vapour pressure, high energy storage capacity and a heat transfer coefficient (0.6-1.2 MW/m^2). Its melting temperature is between 220-250°C. This means this system uses electrical resistances to avoid problems of salt solidification.

The molten salt storage system has two tanks: cold tank with the temperature of 290°C, with electrical resistances in the bottom and middle position, and hot tank with the temperature of 380°C heated by HTF from the solar field.

In a 50 MW plant, this system uses 29,000 tonnes of molten salt. The salt flow during the thermal load is about 940 kg/s. Working for 7.7 hours, it absorbs 130 MW of thermal energy from the HTF. During thermal download, the salt flow is 850 kg/s. During a typical download time of 8.5 hours, it is able to transfer 119 MW of thermal energy to HTF.

Backup system (BS). Plants, with or without storage systems, are usually equipped with a fuel backup system that regulates production, giving a nearly constant power generation capacity, especially in peak periods, and guaranteeing adequate HTF temperature for the plant to continue working. Gas is the typical fuel fo the system. It can provide energy to the HTF, to the storage medium, or directly to the power block. Systems with a BS are called hybrid plants.

Fig. 2.36 shows typical power contribution of a hybrid system with TES and BS.

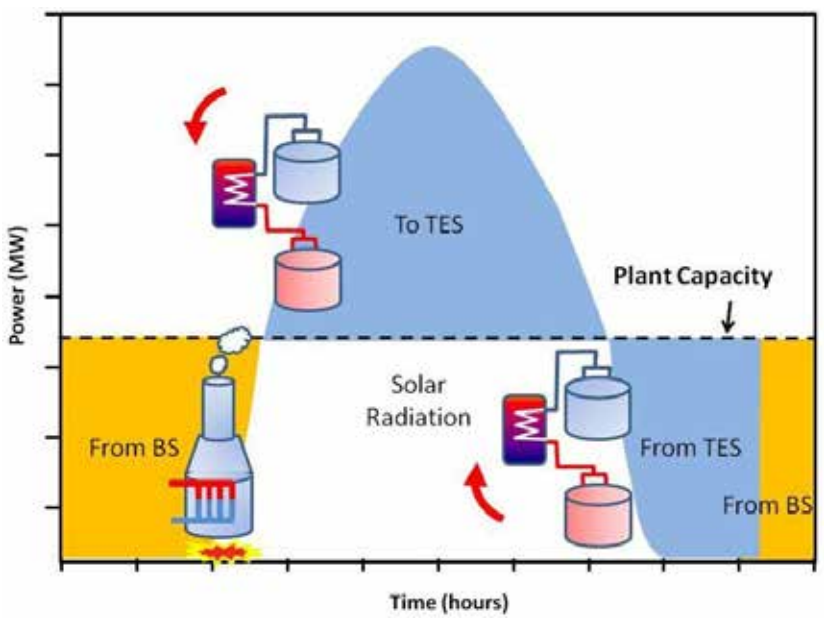

Fig. 2.36. Power contribution of TES and BS in a hybrid PTR plant (Source: own elaboration)

New Technologies in PTR plants

As stated before, the HTF oil cannot reach temperatures above 400ºC with acceptable performance, due to its degradation into unusable components. This limited temperature range is capping the overall steam cycle efficiency. For this reason new technologies with alternative fluids are being researched to reach higher temperatures.

Direct steam generation (DSG): Direct steam generation is considered a very promising option to increase the efficiency of parabolic trough systems, not only because higher working temperatures can be attained in this system, but also owing to the fact that the DSG will permit to directly feed the turbine, hence avoiding the insertion of a heat exchanger and consequently increasing the efficiency (Chiarappa, 2015). Fig. 2.37 shows a simplified scheme of a DSG plant.

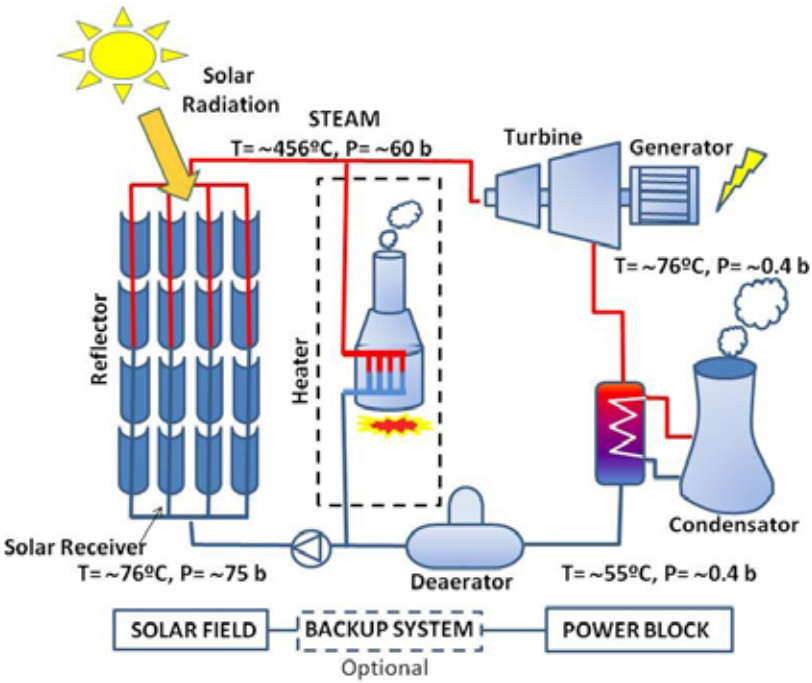

Fig. 2.37. Simplified scheme of a DSG plant (Source: own elaboration)

One of the disadvantages of the DSG system is related to the Thermal Energy Storage (TES) in this system. Traditional molten salt as a storage medium limits the potentiality of the DSG because it imposes a minimum temperature above 240°C which is the solidification temperature for these salts. New technologies are researched to improve the DSG systems, like the Phase Change Material (PCM) storage system. In this system, the latent energy is stored in a sodium nitrate ($NaNO_3$) – a material whose melting temperature is 306ºC (Feldhoff et al., 2012).

According to theoretical calculations, DSG plants could obtain an efficiency of 8% higher than those with synthetic oil. But the investment cost could be 10% higher. This causes about 6% higher levelized electricity costs (LECs) of the DSG system (Feldhoff et al., 2012).

Molten Salt HTF. Molten salt, which is currently used as a heat storage medium, can be used as a Heat Transfer Fluid, reaching temperatures of up to 550ºC. Using molten salt as heat transfer fluid enables a new plant configuration which can lead to savings at several levels:

1) the heat exchange can be eliminated from the storage system, since the fluid that goes from the solar field to the storage system is the same;
2) with the operation at higher temperatures, the molten salt volume for the storage system can be reduced by 2/3, which also leads to a reduction in size of the storage tanks with an impact of 30% reduction in costs.

These savings represent a decrease of approximately 20% of the plant cost when compared with normal oil plants with storage. Also, due to the higher operating temperature, the plant efficiency can increase up to 6%.

Fig. 2.38 shows a simplified scheme of a molten salt plant.

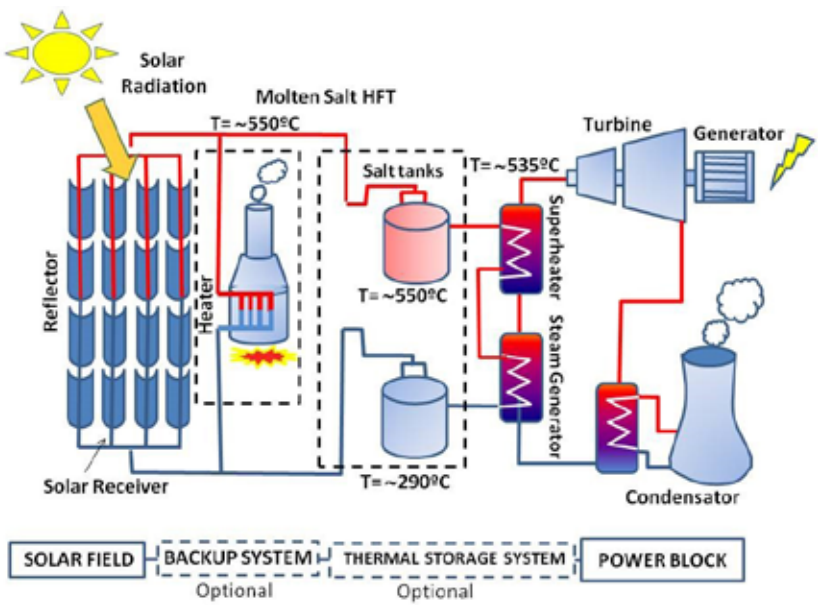

Fig. 2.38. Simplified scheme of a PTR plant with molten salt HFT (Source: own elaboration)

2.5.1.2. Solar tower power plants

This system concentrates the solar radiation in a single point – Central Receiver. Considerably high concentration factor can be obtained which means higher working temperatures and best efficiency of the block power. This technology has yet another advantage: it can adapt to different terrain topographies, it is not restricted to a flat land.

Solar radiation is concentrated by hundreds or even thousands of heliostats (Fig. 2.39), dual-axis tracking concentrator mirrors (flat or slightly curved) that reflect the light to the top of the tower. Currently, heliostats are made with a mirror surface of high optical quality and are 1-140 m^2 in size. A precise tracking system is necessary. Solar tower plants use a linear or rotatory electrical driver to track the sun. Recently, hydraulic drivers are also developed. The sun position is determined by solar tracking algorithms or direct light detection.

Fig. 2.39. Solar tower power plant "GEMOSOLAR" in Cordoba (Source: photo by J. Pastoriza)

Currently, water/steam, molten salt and air are used as HTF.

- **Water/steam technologies** allow steam to be used directly in the turbine to produce electricity without heat exchangers (Fig. 2.40). This is the simplest and oldest technology (First Generation). The problem with this system is that it has no capacity to store energy.
- **Molten salt** is the fluid used usually as heat transfer fluid in next generation of solar tower technologies (Fig. 2.41). The difference is that the system in which molten salt is used allows for storing energy on a cloudy day or at night. The HTF has to be drained from the receiver when the temperatures at the end of day are bellow molten salt freezing temperatures (between 220°C and 250°C), in order to prevent its freezing in the pipes. In this aspect, it should be noted that using molten salt as the HTF is preferred in a solar tower system rather than in a PTR system, as gravity helps the draining of the molten salt. In the case of PTR, pumps are used (Thirumalai, 2014).

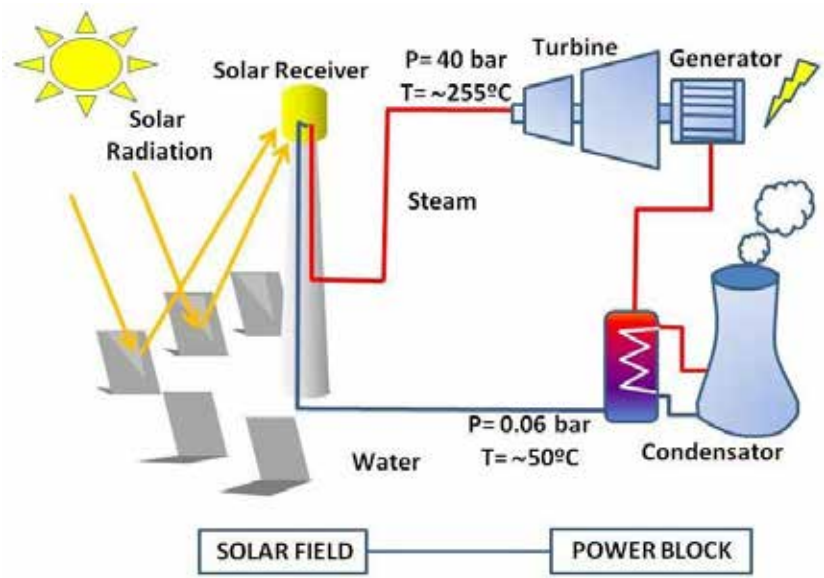

Fig. 2.40. Simplified scheme of a solar tower plant with a water/steam HTF (Source; own elaboration)

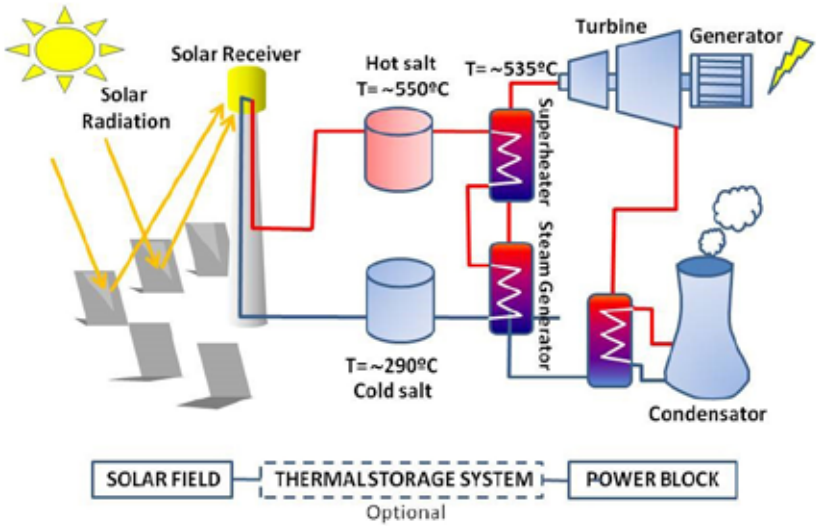

Fig. 2.41. Simplified scheme of a solar tower power plant with a molten salt HTF (Source: own elaboration)

- **Systems with Air HTF** (Fig. 2.42) have disadvantage of its poor heat transfer properties. But it has advantage that allows obtaining temperatures near 1000ºC and requirements of cooling water are lower, that it is very advantageous for countries with water problems.

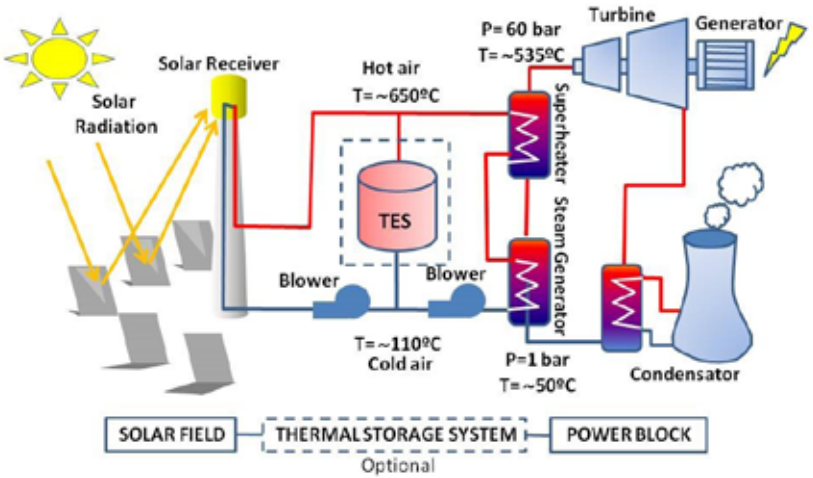

Fig. 2.42. Simplified scheme of a solar tower power plant with Air HTF (Source: own elaboration)

One of the most important parts of solar tower plants is the receiver, which transforms concentrated solar radiation into heat and transfers it to HTF. The type of receiver depends on the HTF used.

There are two main types of receivers:

- **Tubular receivers**, where fluid flows through black-coated tube made of a high-temperature resistant alloy. This type is used for water, molten salt or synthetic oil as the HTF.
- **Volumetric receivers**, where the HTF flows through highly porous wire mesh or metallic/ceramic foams. This type is used for the air or CO_2 as the HTF. There are two types of volumetric receivers: an open volumetric one, in which ambient air is sucked through the porous receiver where it gets heated up by concentrated solar energy, and a close/pressurised volumetric one, in which the HTF is mechanically injected by a blower into the receiver, sealed by a transparent glass. This also allows for increasing the air pressure. As has already been proved, the compressed air has better heat transfer properties.

New technologies in solar tower power plants

The dense particle suspension (DPS) consists of very small particles which can be fluidized with low gas flow. These fluidized particles can be transported to/from tower in manner similar to a gaseous fluid. The DPS is an alternative to the classical HTFs used in solar tower plants. This fluid combines good heat transfer properties of liquids, easy transport of gases and has not problems with temperature of solids: freezing at low temperature and heat cracking at high temperatures typical of molten salts (see Table 2.5).

The DPS system allows for a bigger range of operating temperatures than other HTFs with the improvement of corresponding thermal conversion efficiency of power block. The operating temperature range can be increased by 25% and the efficiency may increase by 40% to 45%. Also, storage temperatures are higher, which means that storage volume can be reduced with similar results. Storage density in this system increases to 13% and a 22.5% reduction in the total storage volume is obtained (Spelling et al., 2015).

Table 2.5. Physical characteristics of the DPS fluid (Source: own elaboration based on Spelling et al., 2015)

Physical Property	Value
Fraction of particles	40% by volume
Density	Above 1000 kg/m^3
Heat transfer coefficient	500-700 W/(m^2·K)
High temperature	Above 650ºC

Fig. 2.43 shows a scheme of solar tower power plant based on the DSP as heat transfer fluid.

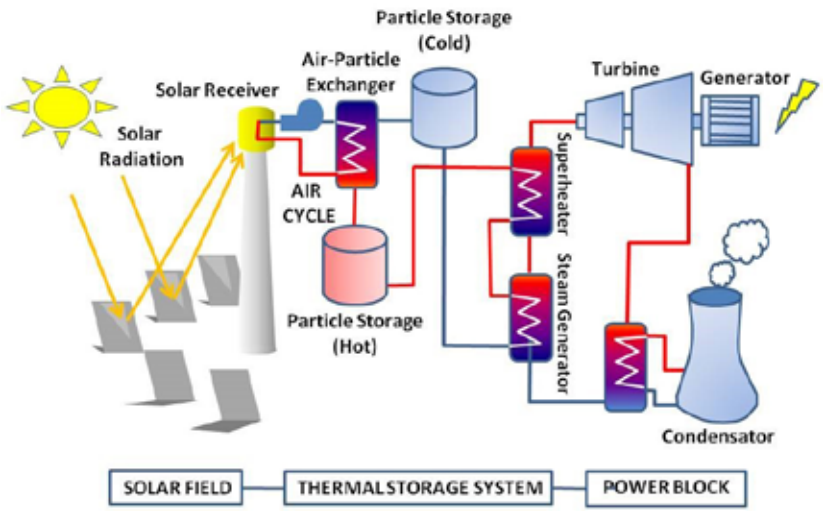

Fig. 2.43. Simplified scheme of a solar tower plant with a dense particle suspension HTF (Source: own elaboration)

2.5.2. Photovoltaic technology

Solar photovoltaic technology converts sunlight directly into solar power (DC electricity) using photovoltaic effect. Solar PV technology is one of the fastest evolving

renewable energy technologies and plays a big role in the global electricity generation market. At the end of 2016, PV capacity reached 303.1 GW, that is 1.8% of the world's total electricity consumption with a continuous exponential growth (Fig. 2.44).

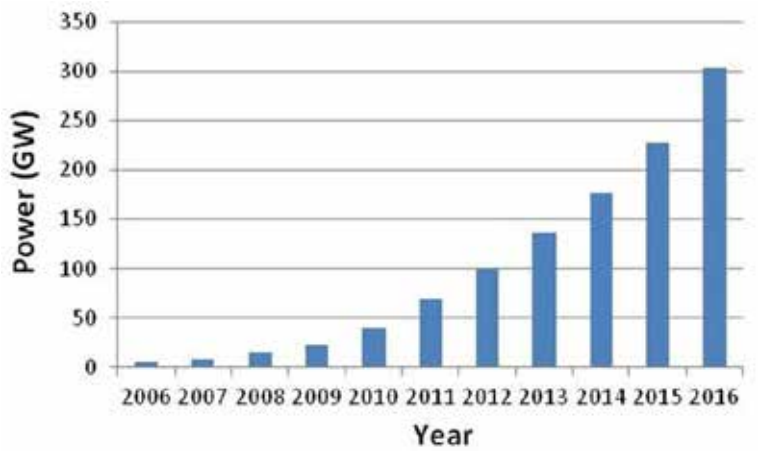

Fig. 2.44. Global Solar PV capacity from 2006 to 2016 (Source: own elaboration based on REN21, 2017)

Asia alone represents around 48% of the total installed capacity. Up to 2012, Europe occupied the first position but since then Asia has grown rapidly. Fig. 2.45 shows generation of top 10 countries.

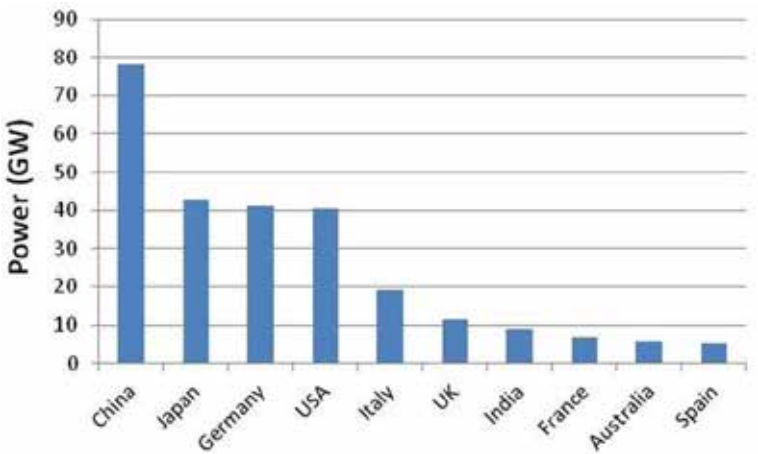

Fig. 2.45. Top 10 countries in 2016 for cumulative installed capacity (Source: own elaboration based on IEA, 2017)

This increasing generation capacity is associated with the reduction of cost of this technology, especially of manufacturing solar cells.

2.5.2.1. Solar Cells

A solar cell is the key component of any solar photovoltaic system. All solar cells require a light absorbing material which absorbs photons for generating free electrons via the photovoltaic effect. A built-in-potential barrier in the cell acts on these electrons to produce voltage, which in turn is used to conduct electrical current through a circuit. This is made by a junction of p and n doped semiconductors (Fig. 2.46).

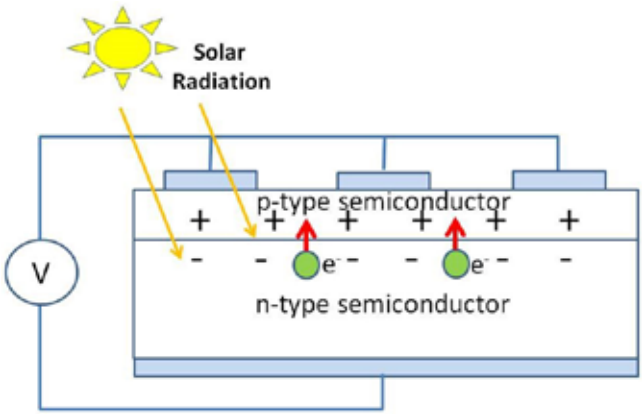

Fig. 2.46. Solar cells. Schematic structure and operation (Source: own elaboration)

Solar cell technology is subdivided into three types: crystalline structure, thin film and compound semiconductor (El-Chaar et al., 2011).

Silicon crystalline structure

The first generation of PV technologies is made of crystalline structure which uses silicon. There are two main types of silicon solar cells:

Monocrystalline solar cells: made from thin wafers of silicon cut from artificially-grown crystals. These cells are created from single crystals grown in isolation, making them the most expensive of the three varieties (approximately 35% more expensive than the equivalent polycrystalline cells), but they have the highest efficiency rating – between 15-24%.

Polycrystalline solar cells: also made from thin wafers of silicon cut from artificially grown crystals, but instead of single crystals, these cells are made from multiple interlocking silicon crystals grown together, hence they are cheaper to produce, but their efficiency is lower than the monocrystalline solar cells, currently at 13-18%.

This technology needs a higher initial investment but the recurrent costs for operation and maintenance are much lower.

Thin film technology

In this technology, thin film cells are created by depositing thin layers of certain materials on glass or stainless steel (SS). The amorphous solar cells may serve as an example.

Amorphous solar cells: instead of using crystals, silicon is deposited very thinly on a backing substrate.

There are two real benefits of the amorphous solar cell; firstly, the layer of silicon is so thin that it allows the solar cells to be flexible and secondly, they are more efficient at low light levels (e.g. during winter). They have the lowest efficiency rating of all three types – approximately 7-9%, requiring approximately double the area to produce the same output.

Other advantages of this technology are lower manufacturing costs due to the high throughput deposition process as well as lower cost of materials.

Compound semiconductor

Cells are made by stacking of crystalline layers with different band gaps that are tailored to absorb most of the solar radiation. Every band gap allows to absorb different portions of wavelength. These hetero-junction devices layer various cells with different band gaps which are tuned utilizing the full spectrum. This technology gives highest efficiency. Multi-junction of Gallium arsenide (GaAs)/indium gallium phosphide (InGaP) has reached 39% (Fig. 2.47).

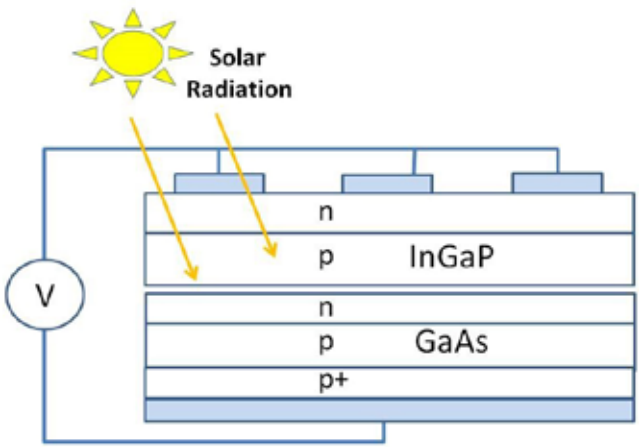

Fig. 2.47. Compound Semiconductor (Source: own elaboration)

2.5.2.2. Solar Modules or Panels

The voltage of a solar cell is low, therefore to reach the necessary operation voltage, a group of cells connected in series is needed. This grouping of solar cells is called PV module or panel (Fig. 2.48).

Fig. 2.48. PV modules in Technologic Campus Rabanales 21 – Córdoba (Source: photo by A. Rodero)

Since the efficiency of the cells is not the same, a breakdown in the cells can occur. At their extreme, such effects can cause destruction of the module resulting from overheating. To avoid this type of problem, protection diodes are installed in every panel.

A window of low-iron high transmission glass protects the surface of the PV material.

2.5.2.3. PV installations

In case of domestic installations two different scenarios need to be considered.

The first one is the PV installation to operate independently (off-grid; not connected to the grid) when the location is remote or far away from the nearest power net. This installation needs PV modules, a load controller/inverter and a storage system (batteries usually).

The second one is the grid-tied PV system as the support to reduce the electricity consumption from the power net. It needs PV modules and load controller /inverter with the interconnection system to the grid.

Fig. 2.49 shows the standard structure and components of a photovoltaic grid-tied system.

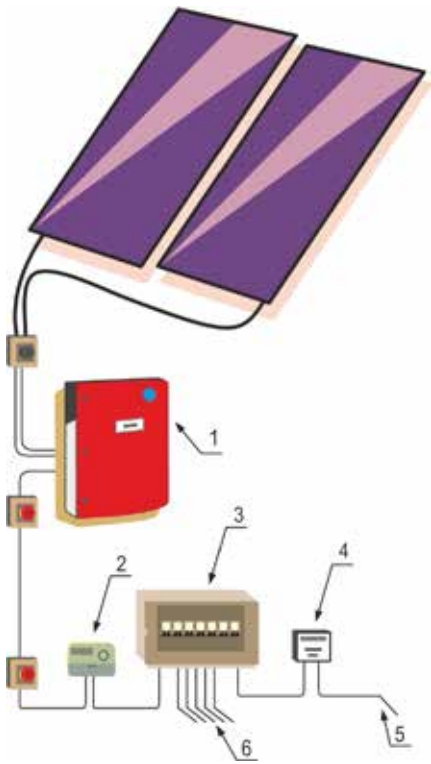

Fig. 2.49. Standard structure of a photovoltaic grid-tied system: 1 – Inverter, 2 – Generation Meter, 3 – Distribution Board, 4 – Electricity Meter, 5 – To the Grid, 6 – Electricity Supply (Source: own elaboration)

2.5.2.4. Solar PV inverters

All the electricity produced by the solar panels is delivered as direct current (DC). The electricity distributed through the grid which we use in our homes is alternating current (AC). For this reason, most solar photovoltaic systems are now connected up to some type of inverter, which changes the DC to AC, allowing the individual to sell the electricity back to the grid (in grid-tied systems) or to be used easily in the houses.

There are maintenance costs associated with the solar PV installation, including cleaning them at least twice a year to ensure they are working as efficiently as possible. In addition, despite the solar panels having a half-life of 25 years, the inverters have a lifespan of about 10 years.

References

Abdelhai, A. (coord.) (2015) *Integrating Solar Thermal in Buildings – A quick guide for Architects and Builders.* United Nations Environment Programme (UNEP) [Online] Available from: http://www.estif.org/fileadmin/estif/content/publications/downloads/UNEP_2015/unep_report_final_v04_lowres.pdf [Accessed 10th August 2018].

Antonelli, M., Baccioli, A., Francesconi, M., Desideri, U. & Martorano, L. (2015) Electrical production of a small size Concentrated Solar Power plant with compound parabolic collectors. *Renewable Energy*, 83, 1110-1118.

Buker, M. S. & Riffat, S. B. (2015) Building integrated solar thermal collectors – A review. *Renewable and Sustainable Energy Reviews*, 51, 327-346.

Burlafinger, K., Vetter, A. & Brabec, C. J. (2015) Maximizing concentrated solar power (CSP) plant overall efficiencies by using spectral selective absorbers at optimal operation temperatures. *Solar Energy*, 120, 428-438.

Chapman, A. J. (1984) *Transmisión del calor*. 3rd Edition. Madrid, Bellisco.

Chiarappa, T. (2015) Performance of Direct Steam Generator Solar Receiver: Laboratory vs Real Plant. *Energy Procedia*. [Online] 69, 328-339. Available from: https://doi.org/10.1016/j.egypro.2015.03.037 [Accessed 10th August 2018].

Duffie, J. A. & Beckman, W. A. (2013) *Solar Engineering of Thermal Processes*. 4th Edition. Hoboken, John Wiley & Sons.

El-Chaar, L., Iamont, L. A. & El-Zeinb, N. (2011) Review of photovoltaic technologies. *Renewable and Sustainable Energy Reviews*, 15(5), 2165-2175

El-Gharbi, N., Derbal, H. & Bouaichaoui, S. (2011) A comparative study between parabolic trough collector and linear Fresnel reflector technologies. *Energy Procedia*. [Online] 6, 565-572. Available from: https://doi.org/10.1016/j.egypro.2011.05.065 [Accessed 10th August 2018].

EnergyPlus (2016) *EnergyPlus Version 8.7 Documentation. Engineering Reference*. U.S. Department of Energy.

Feldhoff, J. F., Schmitz, K., Eck, M., Schnatbaum-Laumann, L., Laing, D., Ortiz-Vives, F. & Schulte-Fischedick, J. (2012) Comparative system analysis of direct steam generation and synthetic oil parabolic trough power plants with integrated thermal storage. *Solar Energy*, 86(1), 520-530.

Frankfurt School-UNEP Collaborating Centre (2016) *Global Trends in Renewable Energy Investment 2016* [Online] Available from: http://fs-unep-centre.org/sites/

default/files/publications/globaltrendsinrenewableenergyinvestment2016lowres_0.pdf [Accessed 10th August 2018].

García-Casals, X. (2001) *La energía solar térmica de alta temperatura como alternativa a las centrales térmicas convencionales y nucleares*.

Groth, C. C. & Lokmanhekim, M. (1969) Shadow – A New Technique for the Calculation of Shadow Shapes and Areas by Digital Computer. In: University of Hawaii. *Proceedings of 2nd Hawaii International Conference on System Sciences, Honolulu, Hawaii, 22-24 January 1969.*

Hendron, R., Anderson, R., Christensen, C., Eastment, M. & Reeves, P. (2004) Development of an Energy Savings Benchmark for All Residential End-Uses. In: NREL. *Proceedings of SimBuild, IBPSA-USA National Conference, Boulder, Colorado, 4-6 August 2004.*

IEA (2017) *2016 Snapshot of Global Photovoltaic Markets*. Report IEA PVPS T1-31:2017. International Energy Agency – Photovoltaic Power System Programme (IEA-PVPS).

ISO (2013) *ISO 9806:2013. Solar energy – Solar thermal collectors – Test methods.* International Organization for Standarization.

Jebasingh, V. K. & Joselin-Herbert, G. M. (2016) A review of solar parabolic trough collector. *Renewable and Sustainable Energy Reviews,* 54, 1085-1091.

Kalogirou, S. (2009) *Solar energy engineering: processes and systems*. Burlington, Academic Press.

López-Cózar, J. M. (2006) *Energía Solar Térmica*. Manuales de Energías Renovables, 4. [Online]. IDAE. Available from: http://dl.idae.es/Publicaciones/10374_Energia_solar_termica_A2006.pdf [Accessed 10th August 2018].

Martínez-Val, J. M. (2004) *La Energía en sus claves*. Madrid, Fundación Iberdrola.

Matthner, F., Weiss, W. & Spörk-Dur, M. (2015) *Solar Heat Worldwide. Markets and Contribution to the Energy Supply 2013.* AEE INTEC. [Online] Available from: https://www.iea-shc.org/data/sites/1/publications/Solar-Heat-Worldwide-2015.pdf [Accessed 10th August 2018].

REN21 (2016) *Renewables 2016. Global Status Report.* Renewable Energy Policy Network for the 21st Century.

REN21 (2017) *Renewables 2017. Global Status Report. Renewable* Energy Policy Network for the 21st Century.

Siegel, R. & Howell, J. R. (1992) *Thermal Radiation Heat Transfer*. 3rd Edition. Washington, Hemisphere Publishing Corp.

Spelling, J., Gallo, A., Romero, M. & González-Aguilar, J. (2015) A high-efficiency solar thermal power plant using a dense particle suspension as the heat transfer fluid. *Energy Procedia.* [Online] 69, 1160-1170. Available from: https://doi.org/10.1016/j.egypro.2015.03.191 [Accessed 10th August 2018].

Thirugnanasambandam, M., Iniyan, S. & Goic, R. (2010), A review of solar thermal technologies. *Renewable and Sustainable Energy Reviews*,14(1), 312-322.

Thirumalai, N. C. (dir.) (2014) *Global Review of Solar Tower Technology.* Center for Study of Science, Technology and Policy (CSTEP).

Turchi, C. (2010) *Parabolic Trough Reference Plant for Cost Modeling with the Solar Advisor Model (SAM)*. Technical Report NREL/TP-550-47605. National Renewable Energy Laboratory.

Walton, G. N. (1983) *Thermal Analysis Research Program Reference Manual*. National Bureau of Standards.

WEB-1: International Code Council (2018) *Solar Rating & Certification Corporation (ICC-SRCC)* [Online] Available from: https://secure.solar-rating.org/Account/CompanySearch.aspx?ctype=Manufacturer [Accessed 10th August 2018].

WEB-2: Solargis (2018) *Download solar resource maps and GIS data for 180+ countries* [Online] Available from: https://solargis.com/maps-and-gis-data/download/ [Accessed 10th August 2018].

WEB-3: ESTIF (2018) *Publications. Archived Statistics. Solar thermal market in Europe. Trends and marked statistics (2004-2015).* [Online] Availabe from: http://www.estif.org/publications/statistics/archived_statistics/ [Accessed 10th August 2018].

WEB-4: https://energyplus.net/weather

WEB-5: Geographic Information System (GIS) of Bialystok City [Online] Available: http://www.gisbialystok.pl/

WEB-6: RENOVETEC. El fluido térmico HTC [Online] Available: http://www.centralestermosolares.com/el-fluido-termico-htf

Winter, C. J., Sizmann, R. L. & Vant-Hull, L. L. (eds.) (1991) *Solar Power Plants: Fundamentals, Technology, Systems, Economics*. Berlin, Springer-Verlag.

Zhang, H. L., Baeyens, J., Degrève, J. & Cacéres, G. (2013) Concentrated solar power plants: Review and design methodology. *Renewable and Sustainable Energy Reviews,* 22, 466-481.